

REPORT DOCUMENTATION PAGE		1. REPORT NO. NSF/CEE-84081	2.	3. Recipient's Accession No. PB88-128764
4. Title and Subtitle Theoretical and Experimental Studies on Timber Diaphragms Subject to Earthquake Loads, Final Summary Report				5. Report Date December 1984
7. Author(s) S.W. Zagajeski; G.T. Halvorsen; H.V.S. GangaRao; L.D. Luttrell;*				6.
9. Performing Organization Name and Address West Virginia University Department of Civil Engineering Morgantown, WV 26506				8. Performing Organization Rept. No.
12. Sponsoring Organization Name and Address Directorate for Engineering (ENG) National Science Foundation 1800 G Street, N.W. Washington, DC 20550				10. Project/Task/Work Unit No.
				11. Contract(C) or Grant(G) No. (C) (G) CEE7804769
13. Type of Report & Period Covered				14.
15. Supplementary Notes *R.B. Jewell; D.N. Corda; J.D. Roberts				
16. Abstract (Limit: 200 words) The principal objective of this report is to summarize a research investigation into the in-plane shear response of plywood timber floor diaphragms. The in-plane shear force-deformation behavior of several full-scale 16 by 24 and 16 by 16-ft plywood-sheathed timber diaphragms in response to dynamic, and monotonic and cyclic static loading was evaluated. A mathematical model was developed to describe plywood-to-joist interaction. The principal objective of the experimental phase of the second stage of the investigation was to determine how timber diaphragm details influence behavior in response to large, in-plane shear deformations. Details considered include: (1) use of blocking; (2) effect of openings, (3) plywood thickness, (4) use of corner stiffeners, and (5) nail size used in substructure connections. A model based on the finite element method was developed to predict the in-plane shear response of the timber diaphragms tested in the experimental phase.				
17. Document Analysis a. Descriptors Shear properties Wooden structures Structural timber Floors Earthquakes Loads (forces)				
b. Identifiers/Open-Ended Terms				
c. COSATI Field/Group				
18. Availability Statement NTIS		19. Security Class (This Report)		21. No. of Pages 94
		20. Security Class (This Page)		22. Price A05 14.95

TABLE OF CONTENTS

Preface	i
List of Figures	ii
List of Tables	iii
1. Introduction	1
1.1 Background	1
1.2 Review of Previous Research	2
1.3 Objective and Scope	4
2. Experimental Program	9
2.1 Construction Details	9
2.2 Materials	14
2.3 Test Parameters	14
2.4 Instrumentation and Test Procedure	16
3. Experimental Results	25
3.1 General Characteristics of Diaphragm Responses	25
3.2 Model Failure	34
3.3 Rigid Body Displacements	37
3.4 Effect of Diaphragm Conditions on Response	39
3.5 Summary of Results for Test Series I	42
4. Analytical Model and Results	45
4.1 Finite Element Model	45
4.2 Parameter Study Results	56
4.3 Comparison of Analytical and Experimental Results	61
5. Summary, Conclusions and Recommendations	72
5.1 Experimental Phase	72
5.2 Analytical Phase	74
5.3 Recommendations	75
References	79
Appendix	81

Any opinions, findings, conclusions
or recommendations expressed in this
publication are those of the author(s)
and do not necessarily reflect the views
of the National Science Foundation.

PREFACE

This document constitutes the final summary report on the project, "Theoretical and Experimental Studies on Timber Diaphragms Subject to Earthquake Loads," conducted at West Virginia University under sponsorship of the National Science Foundation through Contract No. CEE 7804-769.

Faculty Investigators at West Virginia were Stan W. Zagajeski and Grant T. Halvorsen, Assistant Professors of Civil Engineering, and Larry D. Luttrell and Hota V.S. GangaRao, Professors of Civil Engineering. Graduate Research Assistants on the project were Richard B. Jewell, Donald N. Corda, and James D. Roberts. The Program Manager at NSF was Dr. John B. Scalzi.

A Project Advisory Committee was convened in October 1983, to review the Project at that time, and to provide input on additional phases of the work. The committee was Clarkson W. Pinkham of S.B. Barnes and Associates, Thomas D. Wosser of H.J. Degenkolb and Associates, and Ed Zacker of H.J. Brunnier and Associates.

Research reported herein was conducted during the period from January, 1979 through June, 1983.

LIST OF FIGURES

FIGURE

1.1	Two Cyclic Load Histories	8
2.1	Steel Test Frame with Actual Support Conditions	10
2.2	Out-of-Plane Support with Steel Roller	11
2.3	Cross Section of a Typical Test Diaphragm	12
2.4	Corner Opening Layout and Blocking Details	13
2.5	Layout of Exterior Closure Boards for Symmetric Shear Displacement	17
2.6	Slip and Displacement Gauge Locations and Unblocked and Blocked Spacer Locations	19
2.7	Slip Gauge with Strapping Steel	21
3.1	In-Place Shear Displacement Response	26
3.2	Typical Interpanel Nail-Slip Data	28
3.3	Panel Bearing Effects	29
3.4a	Load Deformation Response of Diaphragm IV at Low Loads	30
3.4b	Load Deformation Response of Diaphragm IV at Higher Loads	32
3.5	Load Displacement Response of Diaphragm II	33
3.6	Load Deformation Response of Diaphragm III	35
3.7	Load Shear Deformation Response of Diaphragm IV	36a
3.8	Rigid Body Displacements	38
3.9	Displacement of Blocked Diaphragm	40
4.1	Link Element	48
4.2	Slip Factors for 8d Nails in 1/2" Plywood	50
4.3	Flow Chart of Solution Scheme	53
4.4	Nonlinear Solution Schemes	55
4.5	Effect of Changing S1 and S2 About Their Reference Values on Displacement of Blocked Diaphragm	60
4.6	Displacement of Unblocked Diaphragm	63
4.7	Slip at Position 1 of Unblocked Diaphragm	65
4.8	Slip at Position 5 of Unblocked Diaphragm	66
4.9	Slip at Position 7 of Unblocked Diaphragm	66
4.10	Displacement of Unblocked Diaphragm Altering S1 Range	67
4.11	Displacement of Blocked Diaphragm	68
4.12	Slip at Position 3 of Blocked Diaphragm	69
4.13	Slip at Position 4 of Blocked Diaphragm	69
4.14	Slip at Position 6 of Blocked Diaphragm	70
4.15	Slip at Position 7 of Blocked Diaphragm	70
A-1	Diaphragm Layout	85
A-2	Force Transfer	86
A-3	Building Dimensions	86

LIST OF TABLES

TABLE

2.1	Characteristics of the Diaphragms in Test Series II	18
4.1	Effect of Poisson's Ratio on Diaphragm Displacement	58
4.2	Effect of Young's Modulus on Diaphragm Displacement	59
4.3	Effect of Plywood Thickness on Diaphragm Displacement	59

1. INTRODUCTION

1.1 BACKGROUND

As a structural material, wood is relatively inexpensive and possesses a high strength-to-weight ratio when compared to materials such as steel and reinforced concrete. These characteristics, in conjunction with the relative ease with which it may be handled, cut and connected, make wood one of the principal structural materials in the construction of residential and low-rise building structures in the United States.

A common use of wood in such construction is for roof and floor systems, generally composed of wood joists and plywood panels connected by metal fasteners. The resulting composite structural component serves two principal functions - to transfer gravity loads to vertical load-bearing elements, and to act as horizontal diaphragms which transfer in-plane shear forces to structural elements resisting lateral loads.

The gravity load behavior of plywood-sheathed, wood joist floor systems has been studied extensively as part of a recent research effort at Colorado State University. The results of experimental* (1) and analytical (2) phases of this investigation have quantified the major parameters influencing floor behavior in response to gravity loads, and have demonstrated the benefits of considering the composite nature of this structural system in design (3).

The behavior of a wood floor (or roof) system in response to in-plane shear forces (diaphragm behavior) is of particular concern in situations where wind and/or earthquake ground motion may be significant design considerations. The high in-plane shear stiffness, which is characteristic of typical diaphragms, provides an effective means to distribute the lateral

*Numbers in parenthesis refer to the List of References.

forces associated with wind and seismic load environments to the structure's lateral load resisting elements (4). The performance of timber diaphragms which have experienced recent earthquake ground motion (5), however, has indicated that strength requirements for connections between the timber diaphragm and lateral load elements need to be established. The desired strength requirements may be found by quantifying diaphragm in-plane skew response.

Although the timber diaphragm has been a common solution to the in-plane shear transfer problem in residential and low-rise building construction, the lack of detailed information regarding the behavior of this structural system lead to the initiation in 1978 of research at West Virginia University. Of particular interest in this investigation was the in-plane shear deformation characteristics of timber diaphragms in response to cyclic load reversals which may be expected during earthquake ground motions. A summary of the results of this study are presented in this report. Further details can be found in the thesis and two problem reports prepared by the Graduate Assistants funded through the project (6-8)

1.2 REVIEW OF PREVIOUS RESEARCH

The in-plane behavior of timber diaphragms has been examined by a number of investigators in recent years. These investigations have examined the experimental behavior of timber diaphragms as well as focused on the analytical prediction of response. A review of several of these research efforts is presented below.

Tottenham (10) modeled the interaction of plywood and joists as a series of connected T-beams, introducing a definition of effective flange width. In this model, the diaphragm is idealized as orthotropic and equations are derived for semi-infinite and finite width members subjected to edge shear loads.

Bower (11) examined the deflection of timber diaphragms with complicated shapes, loadings, and/or interfacing elements not covered by present design procedures. In this study, particular attention is paid to the influence of total joint slip within the diaphragm on overall response.

Gulkan, Mayes, and Clough (12) examined the load transfer mechanism in roof diaphragms by subjecting timber roof connections to cyclic loads. Dynamic loading was applied by subjecting a model structure, which included a roof diaphragm, to a simulated earthquake ground motion by means of a shaking table. The model structures were constructed according to standard Uniform Building Code (13) design specifications, and subjected to both in-plane and gravity loads. The factor of safety computed with respect to existing design standards was found to be adequate for connections at both bearing and non-bearing walls.

Ewing, Healey, and Agbabian (14) studied the behavior of timber diaphragms supported on masonry walls and subjected to cyclic loading. The results indicate that diaphragm response is highly nonlinear, and that a low amplitude test is not adequate if diaphragm response in a high seismic area is to be predicted.

One conclusion of previous studies into the in-plane shear behavior of timber diaphragms is that nail slip is the most critical factor of the diaphragm. Consequently it will have a significant effect on response. Therefore, to adequately quantify diaphragm response, an accurate description of nail slip behavior is necessary. A number of experimental studies have been carried out, as well as a number of mathematical models developed to examine nail slip in wood. A summary of these studies follows.

Kuenzi (15), conducted a series of tests and developed a mathematical model representing the nail as a beam on an elastic foundation. Wilkinson (16,17)

expanded Kuenzi's work and developed simple empirical equations relating load to deflection for three cases involving two-member joints:

*Members made of different density materials.

*Joints where one member is relatively thin.

*Members made of similar material types.

It should be noted that Wilkinson's equations were developed on the assumption that each of the members making up a nailed joint have constant Young's moduli through their depth. However, because of the nature of plywood, the Young's modulus across any section of the plywood thickness varies significantly. Therefore, the applicability of Wilkinson's formulas to plywood is questionable.

As part of the Colorado State University effort to describe the gravity load response of wood floors, McClain (18) proposed a curvilinear load-nail slip relationship which is a function of two empirical constants dependent on the specific gravities of the connected materials. In a subsequent study, Stone (19) utilized the work of McClain (18), Wilkinson (16,17) and Antonides (20) to develop a technique which predicts the empirical constants in McClain's nail-slip relationship accounting for material specific gravity, panel thickness, nail size and intralayer gap.

1.3 OBJECTIVE AND SCOPE

The principal objective of this report is to summarize a research investigation into the in-plane shear response of plywood timber floor diaphragms conducted at West Virginia University. The investigation includes experimental and analytical phases and has been carried out in two stages. This report will concentrate on the second stage of the investigation.

The first stage of the investigation was conducted by GangaRao, Luttrell and Jewell. It has been reported by Jewell (6) with a summary of preliminary

results by GangaRao and Luttrell (9). In the experimental phase of this stage of the investigation, the in-plane shear force-deformation behavior of several full-scale 16 by 24 and 16 by 16-ft plywood-sheathed timber diaphragms in response to dynamic, and monotonic and cyclic static loading was evaluated. In addition, the damping and natural frequency of the experimental diaphragms, as well as the local nail-slip response were evaluated. The local nail-slip study was based on the response of small scale specimens which simulated typical plywood panel-joist connections.

The details of the full-scale experimental diaphragms, as well as the characteristics of the test set-up, are discussed in Chapter 2. Details of the results of this phase of the investigation, which is referred to in this report as Test Series I, are presented in a Thesis by Jewell (6) and summarized in Chapter 3 of this report.

In the analytical phase of the first stage of the investigation, GangaRao and Luttrell (9) developed a mathematical model to describe plywood-to-joist interaction. The physical basis of the model is displacement compatibility at the joist-plywood interface, incorporating the influence of joint slip. A detailed description of the characteristics of the model, as well as comparative results, are presented in Reference (9). A summary of the model is presented in Chapter 5.

The second stage of the investigation was carried out by Halvorsen, Zagajeski, Corda, and Roberts. The principal objective of the experimental phase of this stage of the investigation was to determine how timber diaphragm details influence behavior in response to large, in-plane shear deformations. The details considered include:

- 1) Use of blocking,
- 2) Effect of openings,

- 3) Plywood thickness,
- 4) Use of corner stiffeners, and
- 5) Nail size used in substructure connections.

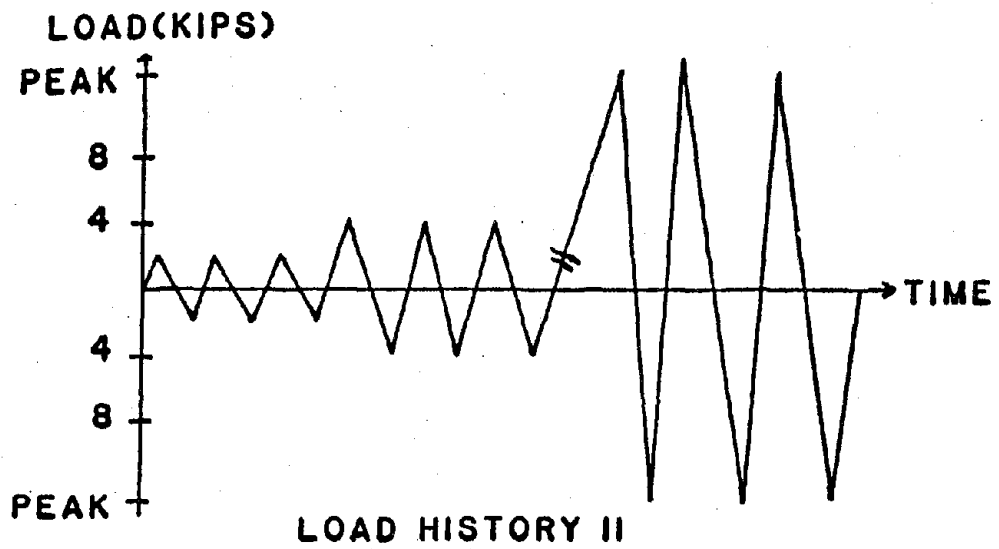
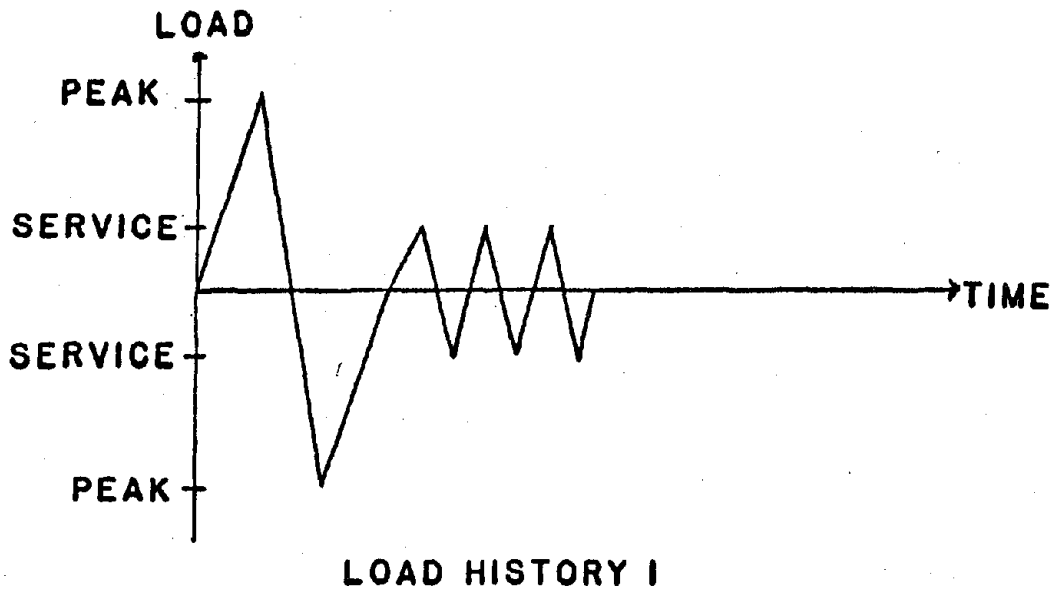
The blocking, corner opening, plywood thickness, and nailing parameters were modified to simulate varying construction details. The corner stiffeners were used to correct a model deficiency (See Section 3.5). A total of six 16 by 24-ft model diaphragms were tested in this stage of the investigation referenced as Test Series II.

An additional factor considered in Test Series II was the effect of load history. Two cyclic load histories were utilized to simulate the in-plane shear induced by earthquake ground motion (See Fig. 1.1). Load history I represents, in an elementary way, a large acceleration pulse occurring during an earthquake ground motion, followed by several service level load cycles. Load history II was considered to examine the effects of cyclic loading over the entire load range.

A detailed discussion of this phase of the investigation is presented in the M. S. Problem Report by Corda (7). A summary of the results are also presented in Chapter 3.

In the analytical phase of the second stage of the investigation, a model based on the finite element method was developed to predict the in-plane shear response of the timber diaphragms tested in the experimental phase of the investigation. In this model, plywood panels are idealized as substructures of plane stress finite elements which are connected by dimensionless link elements included to represent nail-slip between plywood panels. The experimentally observed curvilinear nail-slip response is idealized in the model by a bilinear relationship. A detailed description of this analytical phase of the research is presented in the M. S. Problem Report by

Roberts (8). A summary of the characteristics of the analytical model and analytical results are presented in Section 5.2.



LOAD HISTORIES

Fig. 1.1 Two Cyclic Load Histories

2. EXPERIMENTAL PROGRAM

The timber diaphragms considered as part of this investigation were tested in the Major Units Laboratory at West Virginia University. The test diaphragms were mounted on a 16-6 by 24-6 rectangular steel frame constructed of simply-connected W10x21 members as shown in Fig. 2.1 (Note: the hinge layout of Fig. 2.1 represents the actual support conditions). A schematic representation of these hinges is used in the remaining figures in the report.

The steel frame transferred the load from the hydraulic load activator to the test diaphragm, and served as the boundary element for the test diaphragm. The test frame had virtually zero in-plane shear capacity. The axial capacity of individual members was approximately 40 kips, and out-of-plane support is provided by steel rollers (Fig. 2.2).

2.1 CONSTRUCTION DETAILS

The cross section of a typical test diaphragm is illustrated in Fig. 2.3. The diaphragm construction sequence is as follows: 1) 2x4 (nominal) sections used as sill plates are attached to the steel test frame with 3/4-in. diameter steel bolts spaced at two foot intervals, 2) 2x10 joists are placed on the sill plates at a standard 16 in. spacing, 3) 2x12 closure boards are then installed around the open perimeter of the diaphragm, 4) lateral spacers (blocking) are cut and installed between the joists. In Test Series I blocking was spaced at 5-4 intervals, while in Test Series II, blocking was placed at plywood panel boundaries, as in Figure 2.4. Finally, 5) plywood panels are attached to the substructure (Fig. 2.4). The joists are attached to the closure boards with three 8d or 10d (depending upon the test) common nails. All connections between the plywood and wooden substructure are made with 8d common nails.

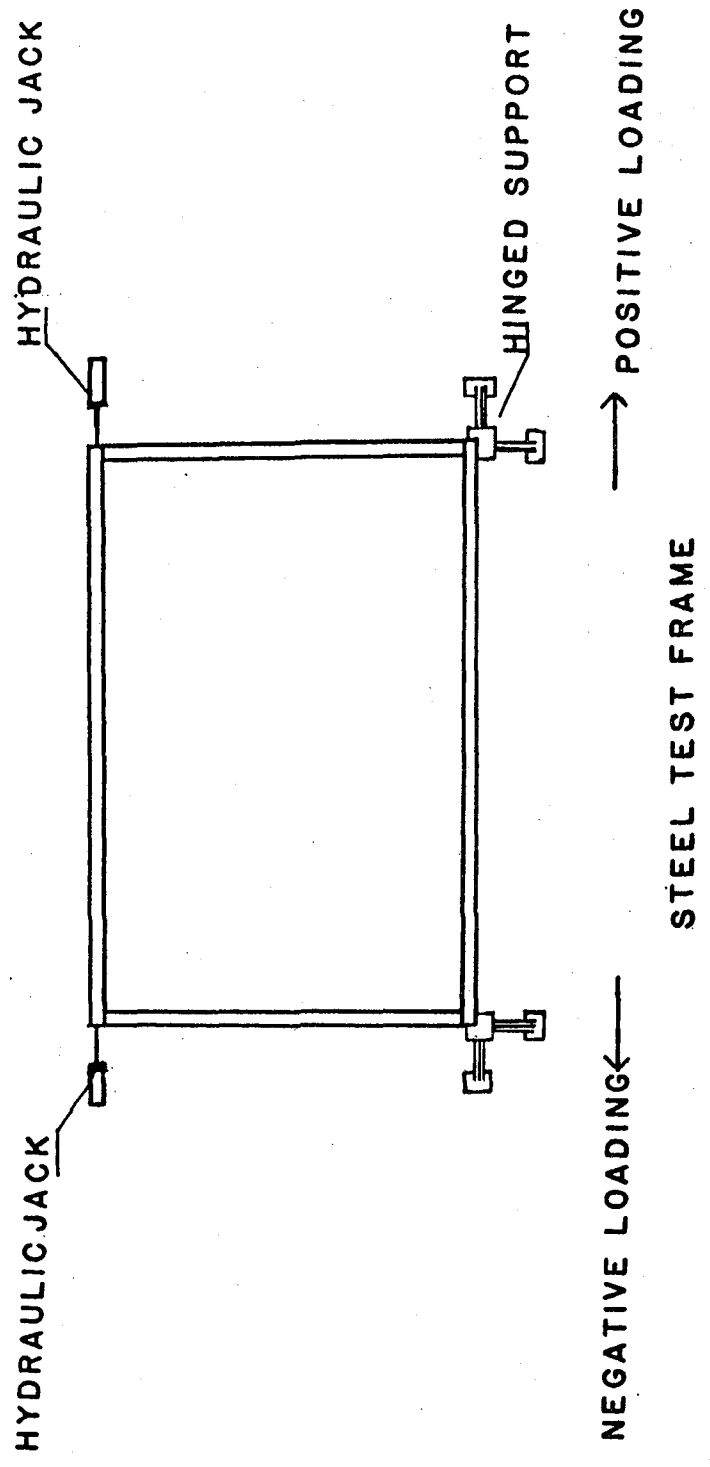
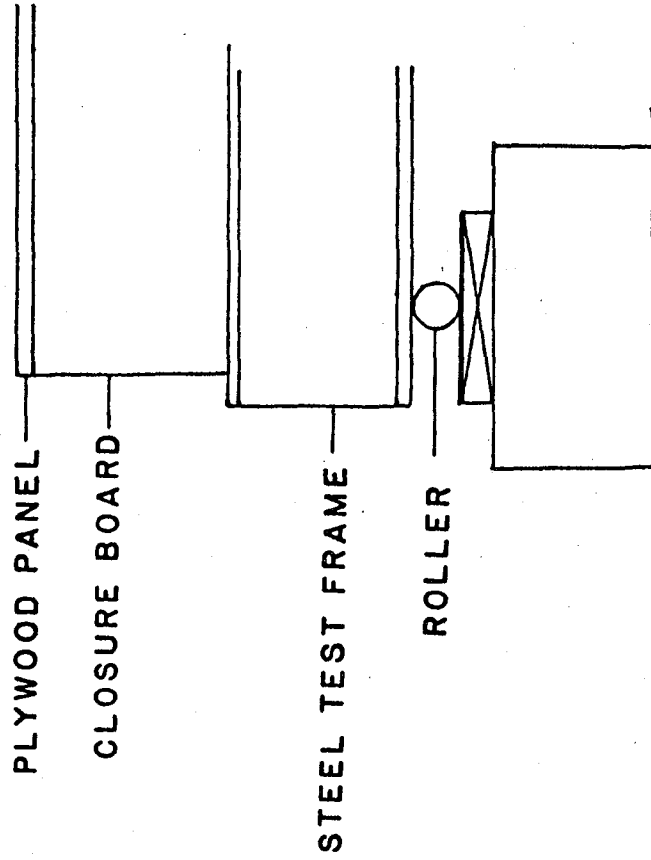
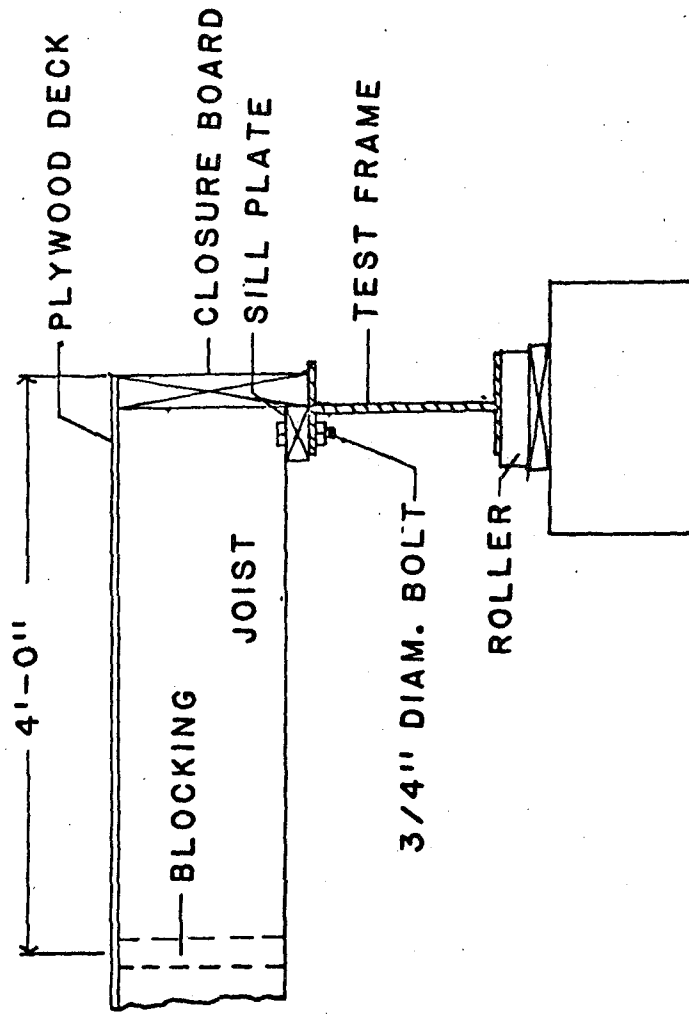


Fig. 2.1 Steel Test Frame with Actual Support Conditions



OUT-OF-PLANE SUPPORT

Fig. 2.2 Out-of-Plane Support with Steel Roller



GENERAL LAYOUT

Fig. 2.3 Cross Section of a Typical Test Diaphragm

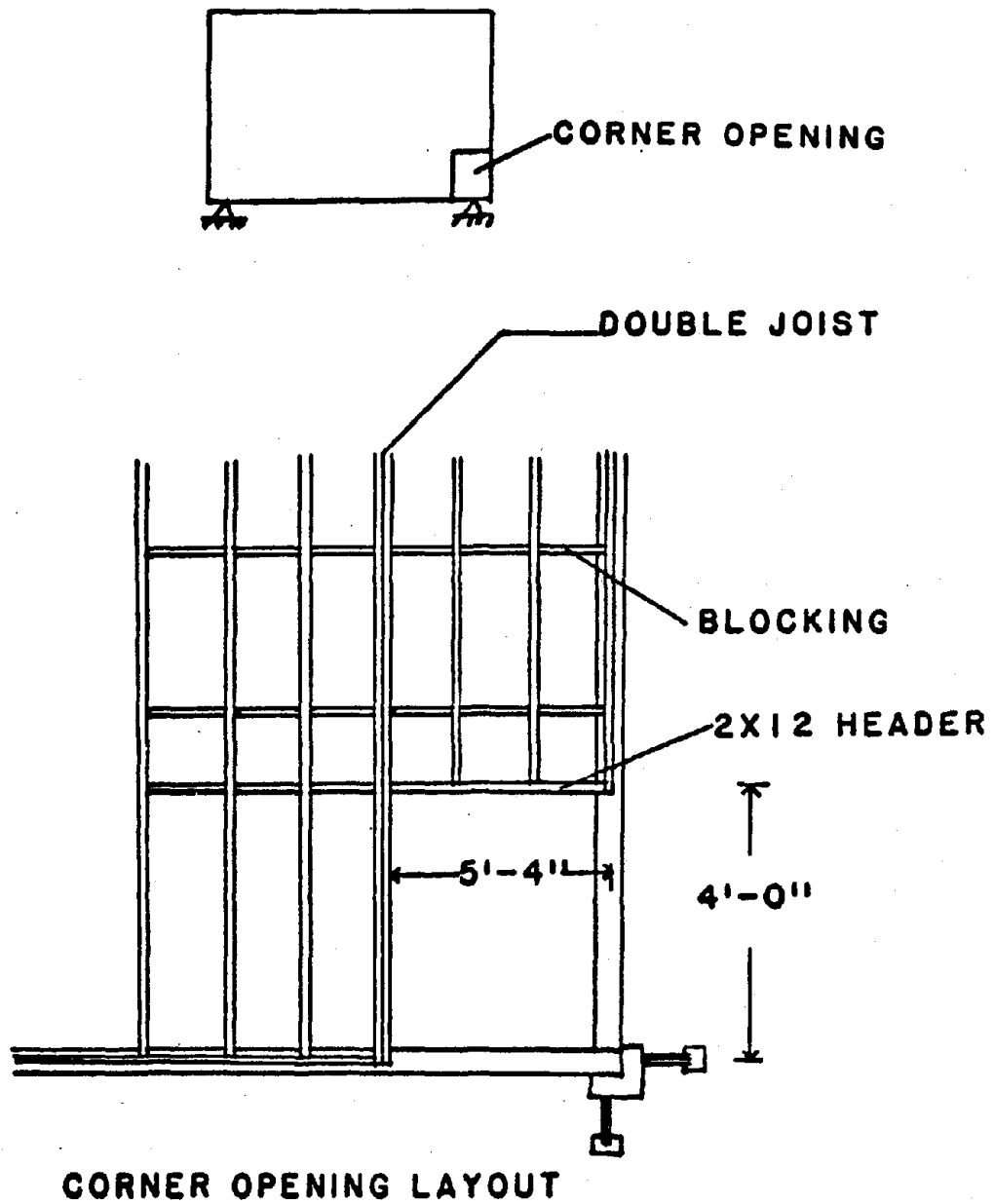


Fig. 2.4 Corner Opening Layout and Blocking Details

All nail spacings used in constructing the Test Series II diaphragms correspond to UBC requirements. The nail spacing for the closure board to sill plate connections and the connections of the plywood sheet boundaries was 6 in. Nail spacing was 12 in. along interior plywood panel boundaries.

2.2 MATERIALS

All materials were of typical construction quality. Framing members were S-P-F No. 2. Plywood panels were C-D exterior grade, as structural grade panels were not readily available. Fasteners were 8d and 10d common nails.

2.3 TEST PARAMETERS

2.3.1 Test Series I

In this portion of the program, a series of experiments were conducted to isolate parametric effects. The parameters investigated were: a) nail spacing; b) diaphragm size; c) boundary conditions; d) diaphragm shape; e) loading type - static, dynamic, impact, load reversal and duration; and f) damping.

For example, full-scale static, dynamic and impact tests were conducted on 16 by 24 and 16 by 16-ft diaphragms. One group of diaphragms was constructed with 2x 10 joist members, whereas another group was constructed with 2x 6 joists. In all cases, the diaphragms were constructed of 1/2-in C-D exterior plywood. The nail spacings used were 4, 6, and 8-in.

A total of 25 tests were conducted by systematically varying the above said parameters. Additional details on diaphragm variables can be obtained from Reference 6.

2.3.2 Test Series II

As noted in the description of diaphragm construction in Section 2.1, the blocking arrangement was changed in Test Series II. In Test Series I, blocking was spaced at 5-4 intervals, its principal function to provide lateral

support for joists. As a result of this blocking arrangement, nail spacing along plywood panel joints perpendicular to the joists was equal to the joist spacing of 16 in. In order to improve the nail-slip characteristics along these boundaries, and consequently improve overall diaphragm shear-displacement response, blocking in Test Series II was placed along all plywood boundaries perpendicular to the joists.

The details of diaphragm I in Test Series II were identical to those of the typical diaphragm used in Series I and tested to familiarize the new investigators with the experimental configuration as well as confirm the results obtained in the first series. On completion of this test, however, the output from the load amplifier in the MTS control used in the experiment was found to be incorrect. As a result, the results obtained are questionable and are ignored in this report.

Diaphragm II was constructed considering standard UBC detailing (13) with nail spacing along plywood panel boundaries equal to six inches. Diaphragm III was similar to diaphragm II with the exception that a 4-0 by 5-4 opening was included. A similar opening was considered in Series I and the results indicated that the discontinuity in stress flow at the opening lead to unacceptable behavior. In an attempt to correct the problem observed in Series I, the corner opening details were modified to reflect suggestions of the Applied Technology Council (21). These details include: 1) placement of a joist along the opening perimeter, 2) use of a 2x12 header at the opening, 3) blocking at the opening interface, and 4) nailing of a metal shear strap between the 2x12 header and blocking at the opening interface (Fig. 2.4). As discussed in Chapter 3, these design details provided an effective means of shear transfer at the corner opening.

Test diaphragm IV was the same as diaphragm II except that the closure

board corner details were modified to achieve a symmetric shear displacement response (Fig. 2.5). The details of diaphragm V were the same as for diaphragm IV except that the plywood panel thickness was changed from 1/2-in (used in all other diaphragms) to 3/4-in. In diaphragm VI, the closure board corner details were again changed to minimize the effects of corner board rotation which lead to failure in diaphragms I-V. The change included installing 4x4 wooden stiffeners at the closure board corner joints and using 10d common nails in substructure framing instead of 8d nails.

A summary of the characteristics of the diaphragms in Test Series II, as well as the cyclic load history considered, is given in Table 2.1.

2.4 INSTRUMENTATION AND TEST PROCEDURE

2.4.1 Load Application and Instrumentation

Test diaphragms in both Series I and II were instrumented to measure applied load, shear displacement, interpanel nail slip, slip between test diaphragm and steel load frame, and support displacement (Fig. 2.6).

In-plane shear loading in test series I was applied at point F by a double acting, servo-controlled, 20 kip capacity MTS actuator. The load magnitude was monitored using a 100 kip load cell, and the corresponding shear displacement was monitored at point A with a dial gage. The resulting load and displacement were recorded manually at selected load increments during the test.

Due to the problem with the load amplifier in the servo-control system mentioned in Section 2.3.2, the double acting MTS actuator was not used in Test Series II. Instead, in-plane shear loading was applied with a single acting, manually controlled actuator placed at either A or F in Fig. 2.6 (placement is a function of load direction). The same 100 kip load cell was used to monitor load magnitude and a linear potentiometer, placed at A in Fig.

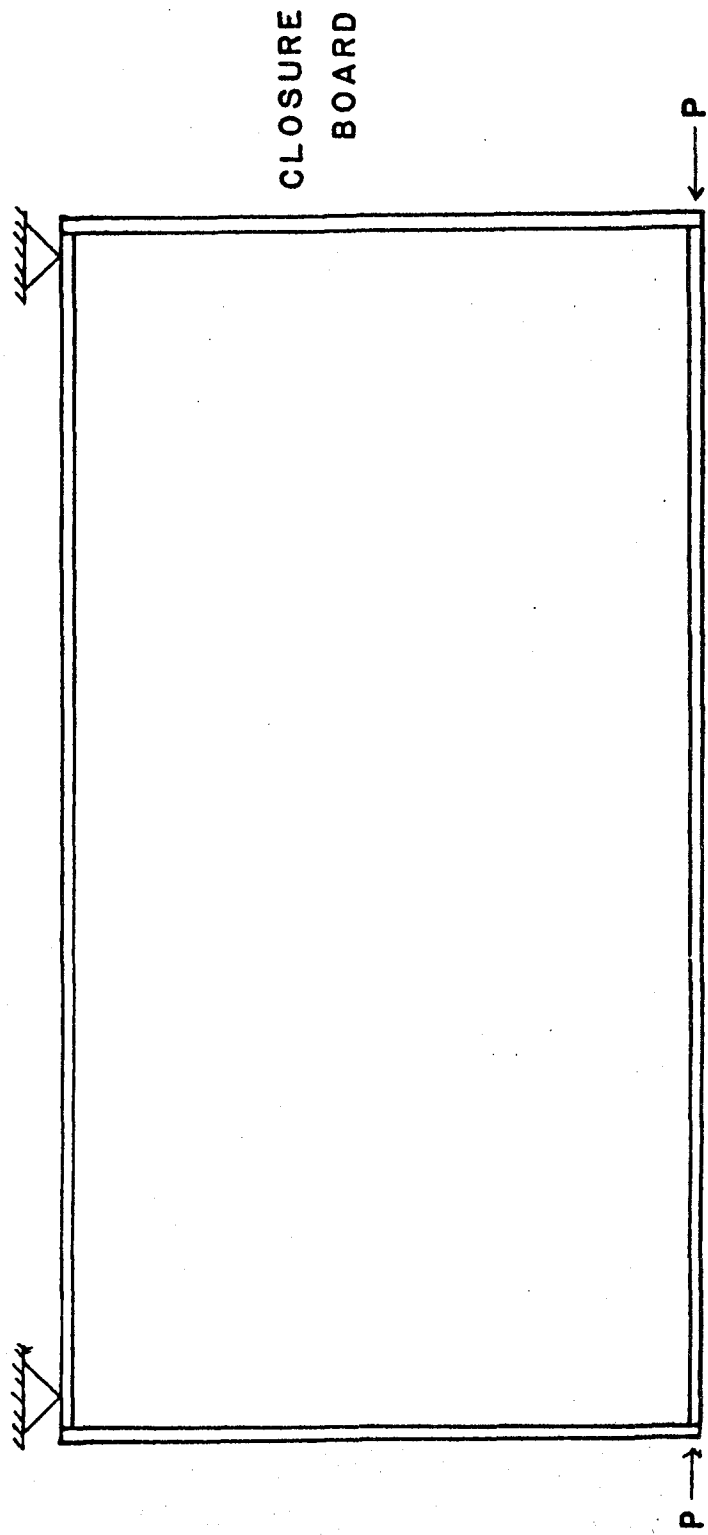


Fig. 2.5 Layout of Exterior Closure Boards for Symmetric Shear Displacement

Diaphragm	Design Parameters	Load History	Load Cycles	Failure Mode
I	"Effective" blocking	Cycle I	±10, ±4	Corner Rotation
II	UBC detailing	Cycle I	±10	Corner Rotation
III	Corner opening	Cycle	±8, ±6, ±4	Corner Rotation
IV	UBC detailing	Cycle II	±2, ±4, ±6, ±8, ±10	Corner Rotation
V	3/4" plywood	Cycle II	±2, ±4, ±6,	Corner Rotation
VI	Corner Stiffeners 10d substructural nailing	Cycle II	±2, ±4, ±6, ±8, ±10	None

Test Summary

Table 2-1. Characteristics of the Diaphragms in Test Series II

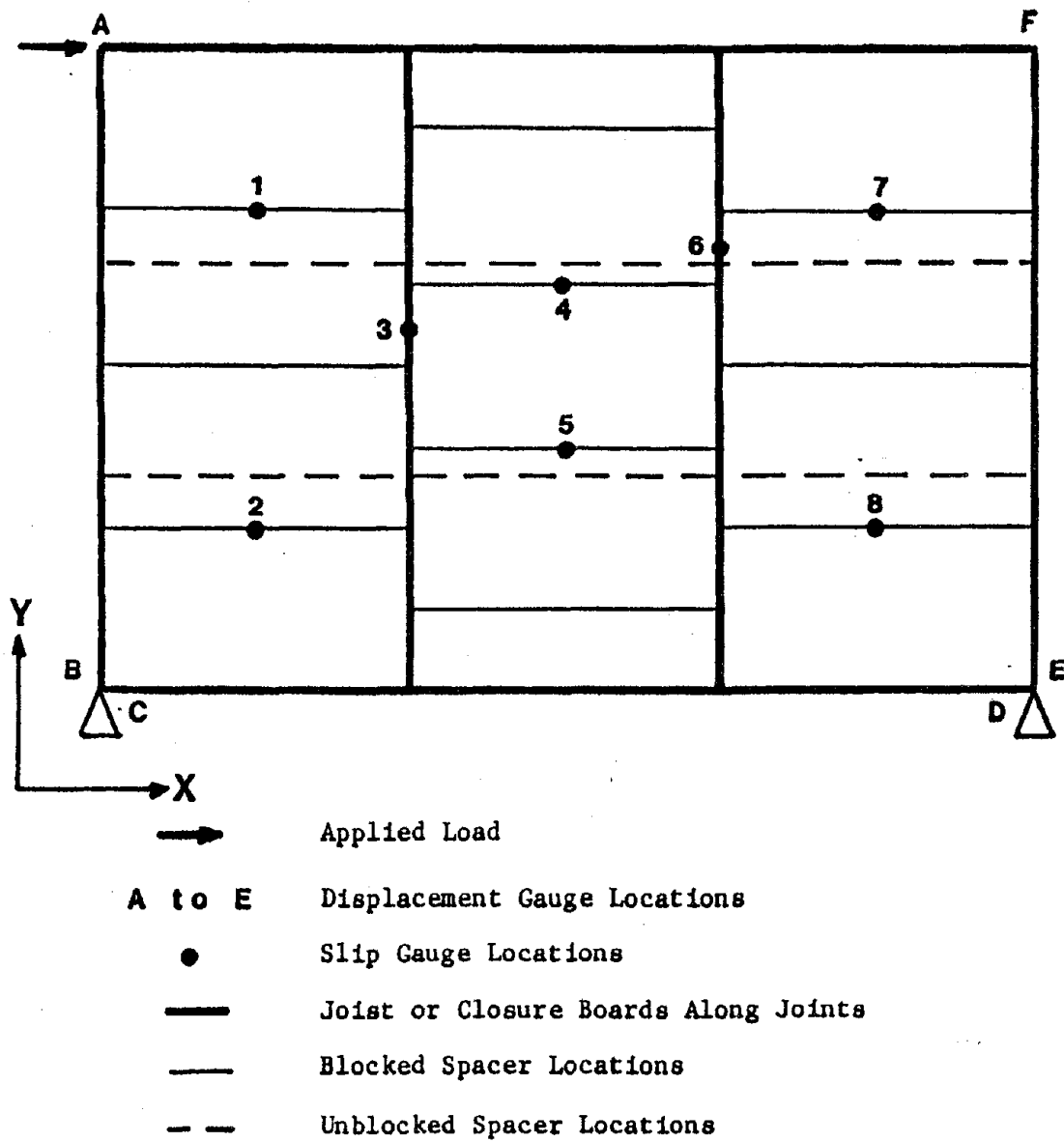


Fig. 2.6 Slip and Displacement Gauge Locations and Unblocked and Blocked Spacer Locations

2.6 was employed to measure shear displacement. The resulting load cell and potentiometer outputs were used as input to an X-Y recorder, thus providing a continuous record of in-plane shear displacement response.

Interpanel nail slip was measured at various diaphragm locations (Fig. 2.6). In Test Series I, spring-loaded dial gages were used to monitor slip, while electronic slip gages were used in Test Series II. The slip gages were developed at West Virginia University and fabricated using a channel-shaped piece of strapping steel. They were instrumented with strain gages arranged to form a full Wheatstone Bridge (Fig. 2.7) Linear calibration curves were obtained for each gage using a calibration block which allowed ± 0.02 in. displacement increments to be applied to the gage. The electronic slip gage data were measured and recorded by a multi-channel strain measurement system, while the dial-gage slip data were recorded manually.

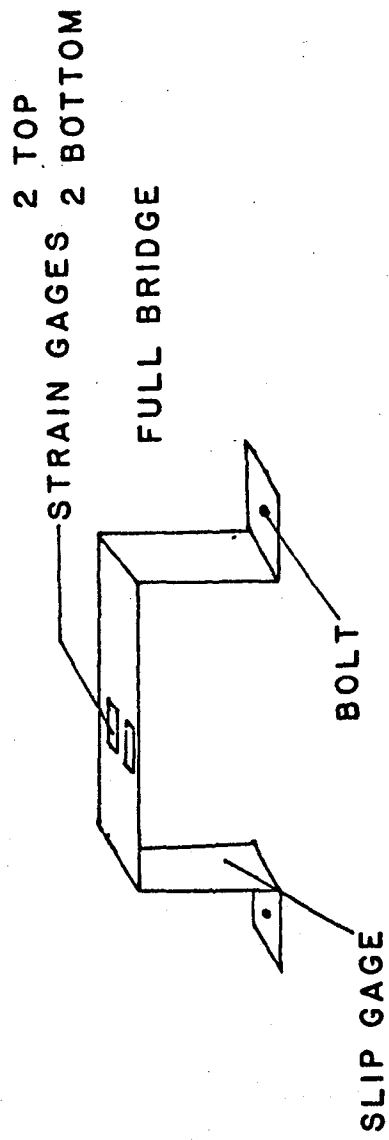
Ames-type dial gages were also used to monitor slip between the diaphragm and steel load frame (at point A in Fig. 2.6), as well as movements at test frame supports (points B, C, D and E in Fig. 2.6).

2.4.2 Diaphragm Loading Test Series I

The method of loading is subdivided into three major categories: static, dynamic and damping. A fourth category consists of miscellaneous loadings which are used to measure diaphragm reaction to certain variables. The diaphragm is tested by in-plane load only; therefore, the capacity of the diaphragm with respect to transverse loads is not considered herein, and all future references to loads will be assumed to be in-plane.

Static Loading

During the static tests, both the hydraulic jack and MTS testing system are used. For the first phase of testing, the manually operated jack is used.



SLIP GAGE

Fig. 2.7 Slip Guage with Strapping Steel

Later on, when the loading cycle is changed, the MTS is used to apply the static load. The first phase of testing consists of applying a positive load to the diaphragm in steps of approximately 0.5 kips to a maximum, and then unloading at approximately the same intervals to a zero load condition. The second phase of static testing, using the MTS, is a modification of the previous procedure. That is, after returning to a zero load condition, the load is applied in the negative direction to a maximum and then is returned to zero in steps. The aforementioned procedure for static testing applied to the large-scale diaphragms while the small-scale joint tests were loaded according to the first phase procedure.

Dynamic Loading

The dynamic phase of testing is, in general, a modification of the static test. The basic procedure is similar to the static test; however, at various load stages the input function is modified. For instance, at 2 kips, the displacement readings are recorded, but instead of increasing the static load, the diaphragm is subjected to a cyclic load. This is done by assigning an input function to the MTS unit. After the period of vibration, the displacement readings are then recorded. Next, the preload is increased to a higher setting and the process is repeated.

It is possible to generate a wide variety of frequencies and load magnitudes but impossible to test the diaphragms under all of these conditions. Therefore, it was decided to use one frequency and one magnitude of loading. Five Hertz was chosen as the frequency and 0.5 kips as the load. The forcing function chosen is sinusoidal. Therefore, the total load at any stage consists of a preload and additive sinusoidal load. This frequency and amplitude has been chosen because the combination provides sufficient movements at the various joints to show a pattern of displacement, yet it is

not excessively destructive. The load is applied over approximately the same range as the static test for each set of parameters.

During the preliminary stages of the test, each sinusoidal load schedule consists of 1,000 cycles. Later in the series, the maximum number of cycles is decreased to 500 cycles per step. The reason for this was discussed in Reference 6.

In order to reduce the effect of impact loading, due to the relatively sudden application of 0.5 kips, the load is increased from zero to 0.5 kips over the first few cycles of the load.

Damping Tests

An important property of the diaphragm is its damping characteristics. Different approaches have been evaluated in an effort to determine the best method of finding a damping value. A constant load, for example 3 kips, is applied to the diaphragm as in the static test through a tension connector (refer to Reference 6 for additional details) or turn-buckle. This connector is cut, suddenly releasing the diaphragm. The structural behavior from this impact condition is recorded on an oscilloscope. Response of this sudden load release has been photographed and analyzed in determining the damping ratio.

2.4.3 Diaphragm Loading Test Series II

As noted in Section 1.3, the effect of large cyclic shear deformations on the in-plane behavior of timber diaphragms was of particular interest in Test Series II. In order to study this behavior, two different cyclic load histories were considered (Fig. 1.1). A brief discussion of each is presented below.

I. Load History I

Diaphragms I-III were subjected to load history I. The loading sequence

considered in this load history (Fig. 1.1a) is as follows: 1) take initial readings at zero load, 2) increase load in increments of approximately two kips until a flattening of the load-displacement response was observed, 3) reduce the loading to zero and take readings, 4) repeat steps two and three with load applied in the opposite direction, 5) repeat steps one through four, two more times for a total of three cycles.

II. Load History II

Diaphragms IV-VI were subjected to load history II. The loading sequence considered in this load history (Fig. 1.1b) is as follows: 1) take initial readings at zero load, 2) load in the "positive" direction until reaching the desired load level, 3) take readings, 4) reduce load level to zero and take readings, 5) repeat steps two through four with load applied in the opposite direction, and 6) repeat steps one through five two more times for a total of three cycles. The basic load sequence started at a load level of 2 kips. The load level gradually increasing in 2 kip increments until diaphragm failure, or until it was impractical to apply additional load.

3. EXPERIMENTAL RESULTS

The results of an experimental program to evaluate the in-plane shear response of timber diaphragms are presented in this chapter. The general characteristics of in-plane shear displacement behavior is first discussed, followed by a discussion of the effects on behavior of the various diaphragm parameters considered as part of this investigation. The discussion of results focuses on global displacement response as well as local slip behavior and model failure.

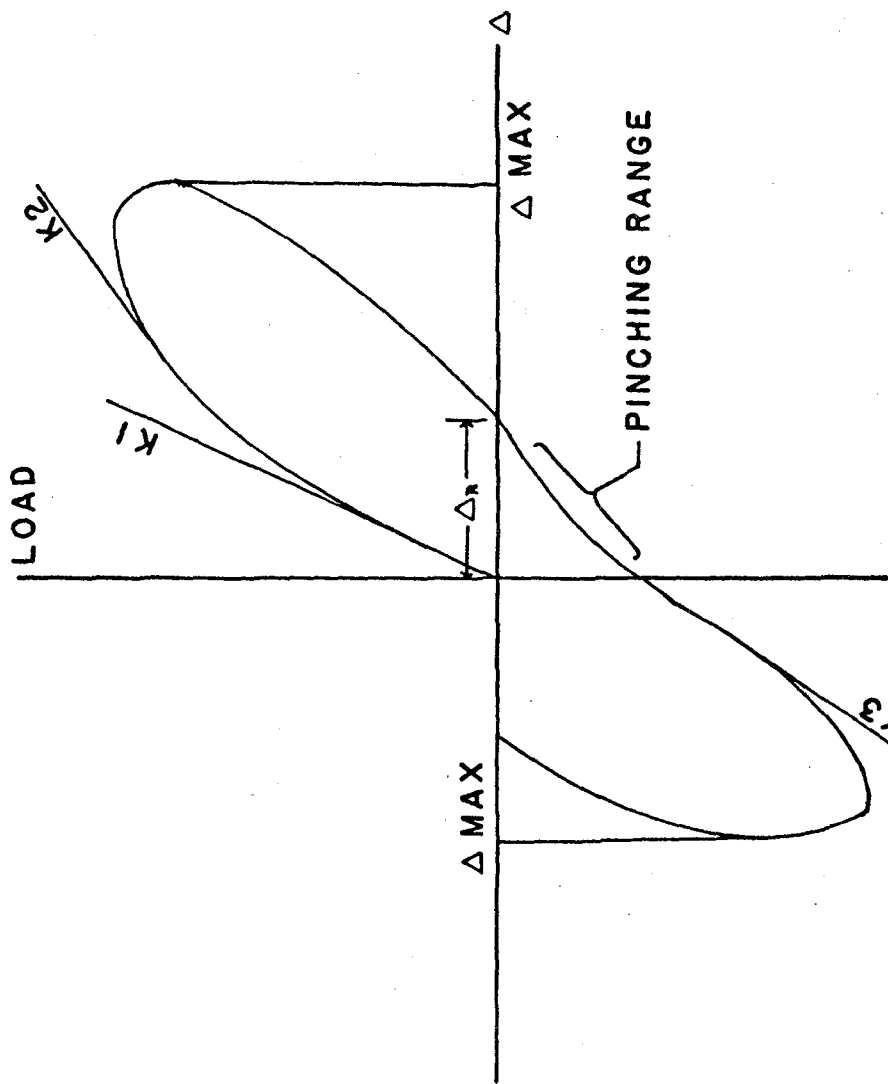
Detailed discussions of the experimental results for Test Series I may be found in Reference (6) and for Test Series II in Reference (7).

3.1 GENERAL CHARACTERISTICS OF DIAPHRAGM RESPONSES

The in-plane shear stiffness of a typical plywood panel in a timber diaphragm is significantly greater than the whole system since the stiffness of nailed joints is a limiting condition. As a result, the response of the diaphragm is analogous to a series of fairly rigid plates connected by flexible joints, and diaphragm behavior is controlled by the shear stiffness of these joints.

The essential features of the in-plane shear displacement response is illustrated in Fig. 3.1. As the shear force is increased from zero, the diaphragm shear stiffness initially remains constant but then experiences a gradual decrease. The decrease in stiffness continues until it approaches zero, at which point the loading was stopped, and the diaphragm was unloaded.

The observed change in stiffness is attributed to a degradation, with increasing load, of nail-slip stiffness between plywood panels. This degradation is associated with local damage to the wood in the vicinity of the connectors, as well as possible inelastic behavior of the connectors. Reducing the load to zero after reaching the force and displacement level indicated in Fig. 3.1, results in a significant residual displacement which is for the most



- K = Initial Stiffness
- K_1 = Reduced Stiffness
- K_2 = Initial Stiffness of load reversal
- K_3 = Residual Displacement
- Δ_R = Maximum Diaphragm Displacement

TYPICAL LOAD-DEFORMATION RESPONSE

Fig. 3.1 In-Plane Shear Displacement Response

part due to the local damage in the nailed joints caused by the initial load application. If at this point, load is applied in the opposite direction, the shear stiffness is initially relatively small. It gradually increases, however, as the load increases until the response is similar, though more flexible, to that observed in the initial load cycle. This pinching phenomenon at the start of the shear displacement response on load reversal is attributed to the slack in nail joints associated with the local damage discussed above. As the load magnitude is increased, this slack is gradually recovered, and the interpanel joint resistance to slip gradually increases.

The apparent degradation in nail slip response is illustrated by typical interpanel nail-slip data given in Fig. 3.2. The slip data locations are defined in Fig. 2.7.

Examination of these slip data indicates that, after an initial constant stiffness response, the nail stiffness gradually decreases with increasing load. In addition, it is observed that slip magnitudes are not constant throughout the diaphragm.

The latter feature of nail-slip response is attributed to the staggered arrangement of the plywood panels in the long direction of the test diaphragms (Fig. 3.3). As a result of this arrangement, application of in-plane shear causes panels to move in groups (for example panels P1, P5, P6, P10 and P11 in Fig. 3.3), and the smaller slip response corresponds to movement within groups (point 7 data in Fig. 3.2), while the larger slip response corresponds to movement between groups (data for points 1 and 5 in Fig. 3.2).

The influence of nail slip response on diaphragm shear displacement behavior is further illustrated by the response of diaphragm IV from Test Series II presented in Fig. 3.4. This diaphragm was subjected to load history II (Fig. 1.1b) in which a series of incrementally increasing load cycles were repeated three times.

Examination of the force-displacement response illustrated in Fig. 3.4a

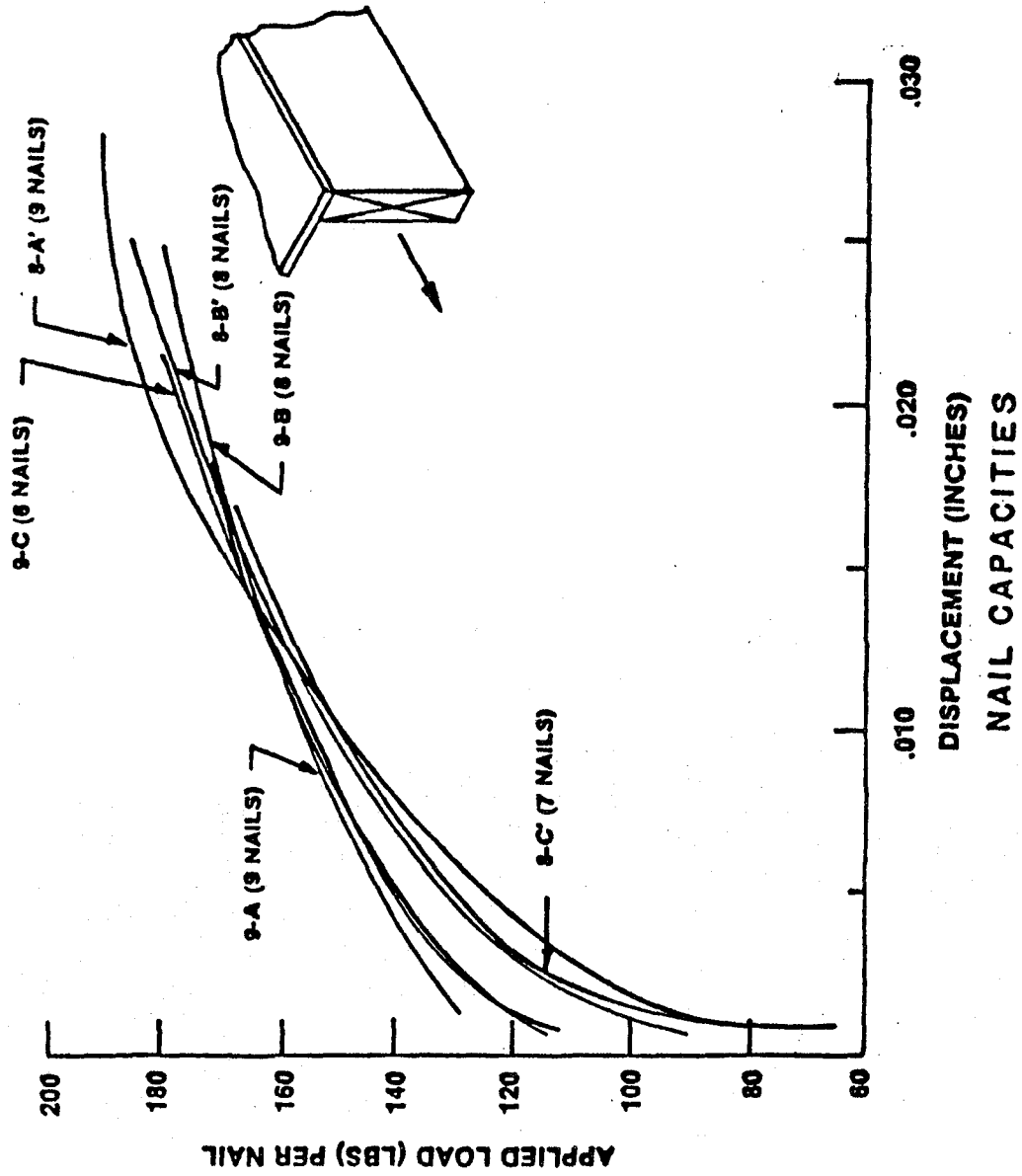


Fig. 3.2. Typical Interpanel Nail-Slip Data

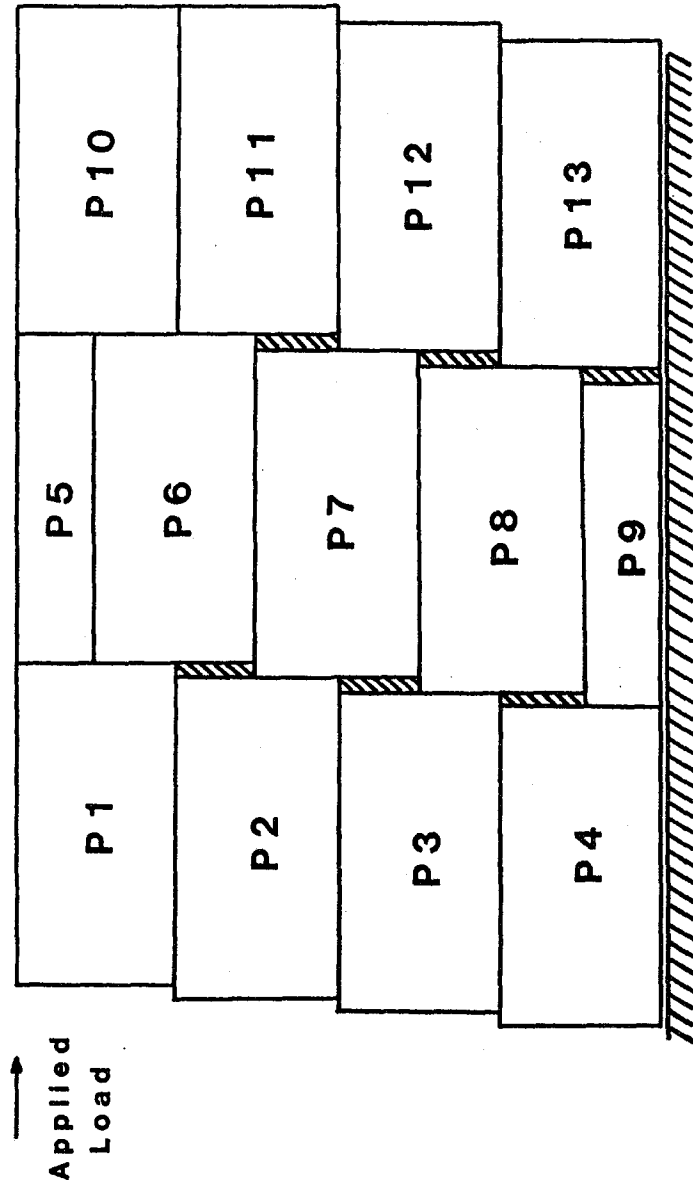


Figure 3.3. Panel Bearing Effects

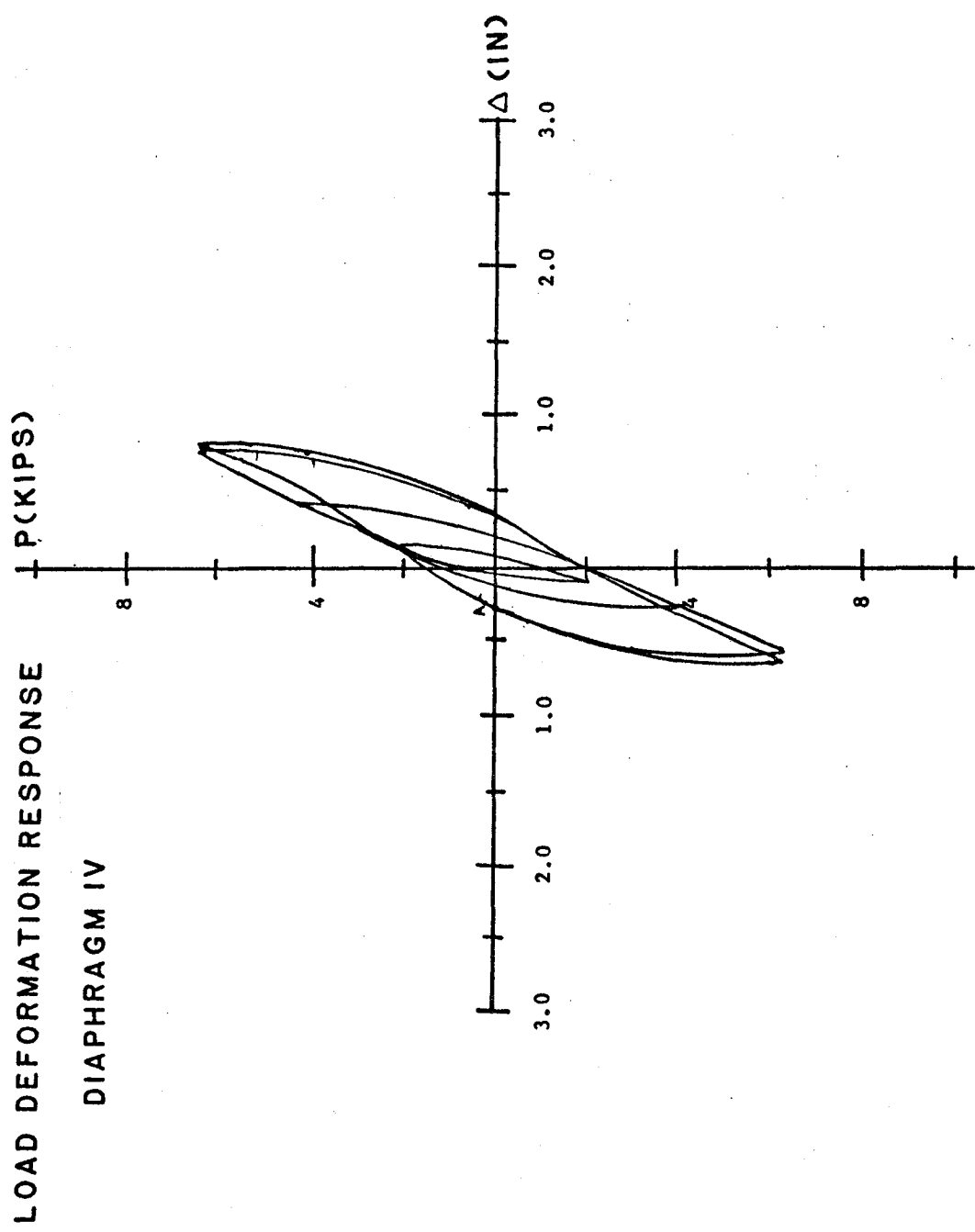


Fig. 3.4a. Load Deformation Response of Diaphragm IV at Low Loads

indicates that at low level load cycling (two and four kip loading); the resulting force displacement loops are essentially the same in either load direction, the loops for each cycle at a given load level overlap, and the pinching phenomenon is not evident on load reversal. These observations lead to the conclusion that degradation of the nail-slip mechanism between plywood panels is minimal at low load levels.

As the cyclic load level increases, one to six kips then to nine kips, pinching becomes evident and cycling at a given load level causes a faster degradation in the shear displacement response.

The observed response degradation is a function of load level. For example, after the first cycle at six kips pinching becomes evident on reversal and in subsequent cycles, indicating local damage to nailed-joints. However, the loops for the second and third cycles overlap, indicating that further damage to the nailed joints does not occur.

This is in contrast to the response for a load level of 9 kips, (Fig. 3.4b) at which the extent of pinching and overall diaphragm degradation increases with each cycle. Consequently, it appears that the damage to nailed joints accumulates with each cycle leading to additional degradation in shear displacement response.

It should be noted that the failure indicated in Fig. 3.4b is not due to a failure of the nail-slip mechanism, but rather a rotation of the closure board at support B-C (Fig. 2.6). In view of this, the cyclic degradation illustrated in Fig. 3.4b is more likely a consequence of deterioration of the closure board corner joint, than degradation of the nail-slip mechanism. This point, as well as model failure are discussed further in section 3.3.

A comparison of the in-plane shear response of test series II diaphragms II (Fig. 3.5) and IV (Fig. 3.4b), which were the same except for the difference in load history and a minor change in the closure board corner detail (Fig. 2.5) indicates a similar degradation in shear stiffness as a result of cycling at 10

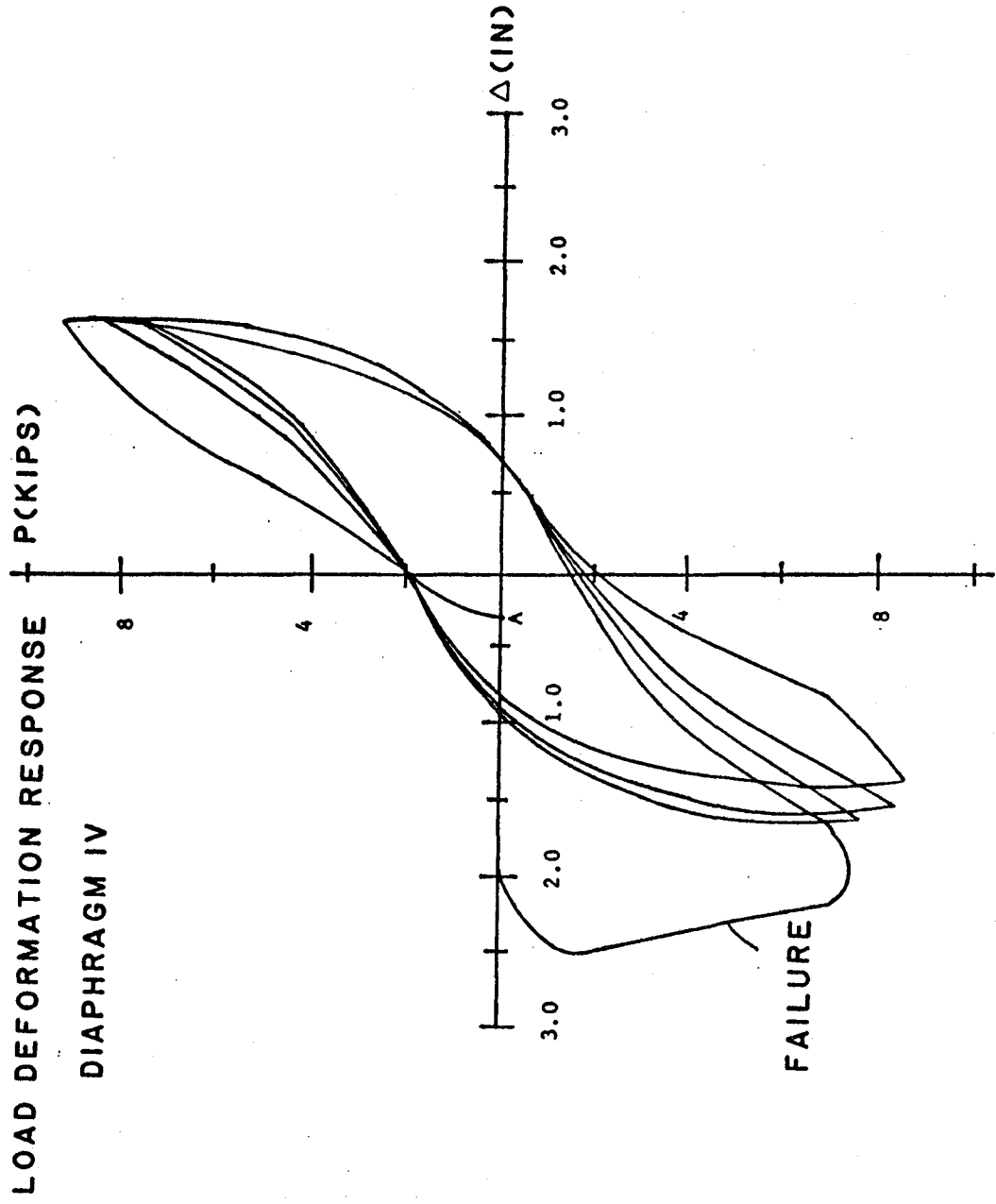


Fig. 3.4b. Load Deformation Response of Diaphragm IV at Higher Loads

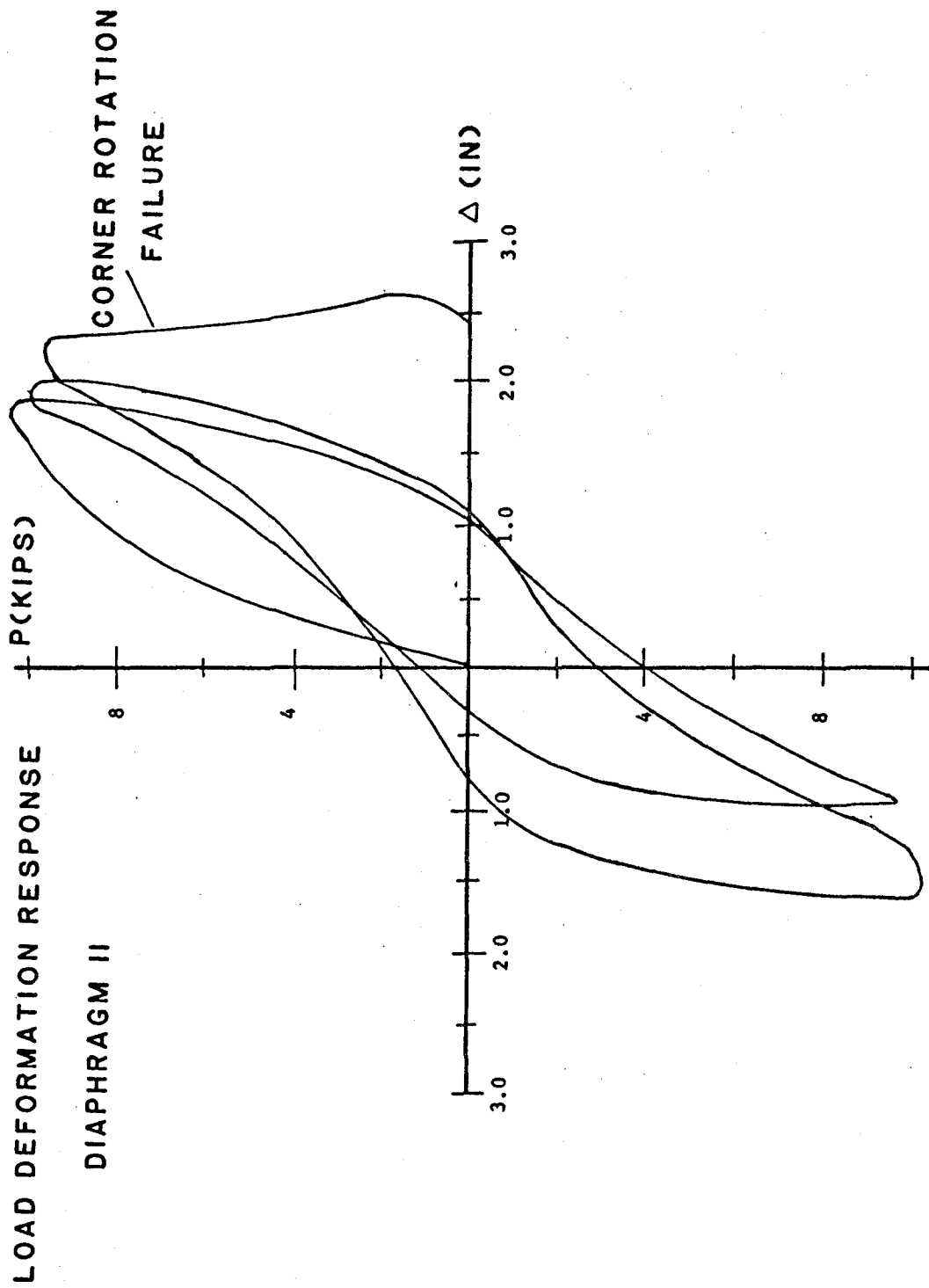


Fig. 3.5. Load Displacement Response of Diaphragm II

and 9 kips respectively. As a result, it may be concluded that load level is the principal factor influencing shear degradation, although previous load history may have a minor influence on the load level at which significant degradation begins.

Examination of the cyclic response of series II diagram III at a load level of 4 kips (Fig. 3.6), which was supplied after the initial peak load cycle of history I, demonstrates that the damage to nailed-joints caused by cycling at a given load level is permanent. In addition, further shear degradation will not occur as a result of cyclic loading at load levels smaller than the previous maximum level.

In summary, the in-plane shear response of diaphragms II, III and IV demonstrates that cyclic nail-slip behavior is nonlinear but stable (i.e. the in-plane shear displacement hysteresis loops at a given load level overlap). When this occurs at high load levels, however, cyclic degradation of in-plane shear response eventually leads to diaphragm failure. Although deterioration of the nail-slip mechanism may contribute to this degradation, the principal cause is believed to be a deterioration of the closure board corner joint connections.

3.2 MODEL FAILURE

As noted in the above discussion, the typical experimental failure is attributed to rotation of the closure boards at a corner of the test diaphragm. This rotation caused the joint between the two closure boards to open, resulting in a sudden loss of in-plane shear strength.

The closure board rotation is attributed to the transfer of in-plane shear forces around the diaphragm perimeter, from the plywood panels, through the closure board, to the sill plate. The eccentricity of this transfer, in conjunction with the stress discontinuity associated with the diaphragm corner, tends to rotate the closure board in such a way that the nailed connection

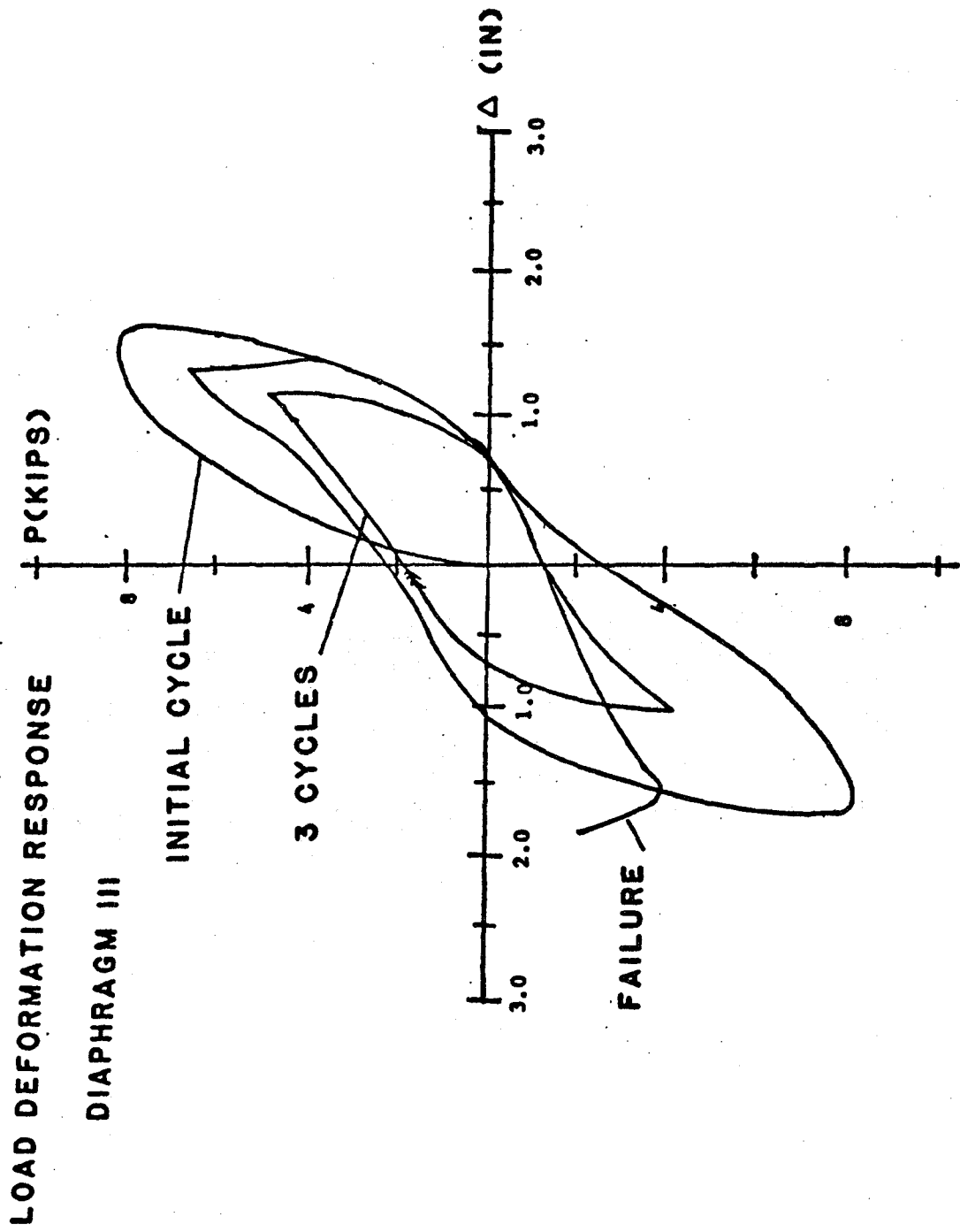
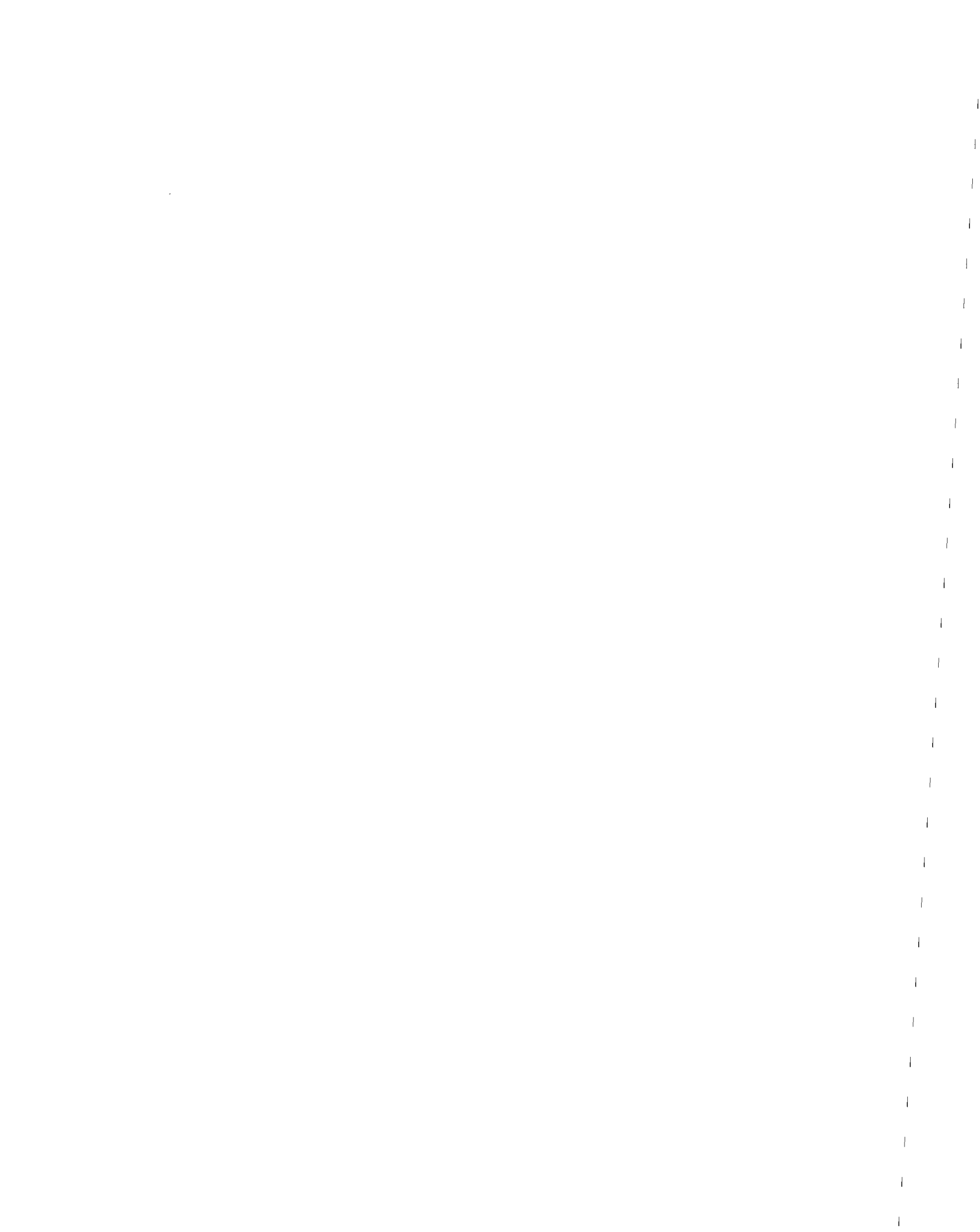


Fig. 3.6. Load Deformation Response of Diaphragm III



between the closure board and sill plate is required to resist tension when the plywood panel pulls on top of the closure board. As the applied shear force is increased, the tension resistance of the closure board, sill plate connections, as well as the closure board corner connection, are exceeded and the closure board corner joint opens.

In an attempt to eliminate this apparent weak point in the experimental diaphragm, the closure board corner detail was modified in diaphragm VI of test series II. The modification included the use of 4x4 wooden blocks to reinforce the corner joint, and increasing the nail size used in substructure framing from 8d and 10d common nails.

The in-plane shear displacement behavior of diaphragm VI at cyclic load levels of approximately 8, 10 and 11 kips is illustrated in Fig. 3.7. The minor cyclic shear degradation indicated in Fig. 3.7 demonstrates the effectiveness of the joint reinforcement and larger substructure nail size in eliminating the problem of closure board rotation. It should be noted that three load cycles of 8 and 10 kips were applied, the last two producing essentially identical responses. In fact, an actual failure was not observed in diaphragm VI since loading had to be discontinued when apparent load eccentricity caused the entire test frame to lift off the out-of-plane supports during the load cycle of approximately 11 kips.

A comparison of the cyclic shear displacement response for diaphragm IV (Fig. 3.4b) and diaphragm VI indicates that the significant shear degradation observed in model IV is primarily a result of the deterioration in the closure board corner joints and not a general degradation of the nail-slip mechanism. Consequently, the accumulated damage referred to in the previous discussion of the behavior of diaphragm IV is damage to the closure board corner joint.

The behavior of diaphragm VI demonstrates that if proper attention is paid to construction details at points of stress discontinuities - in this case corner connection details - plywood timber diaphragms can undergo large cyclic

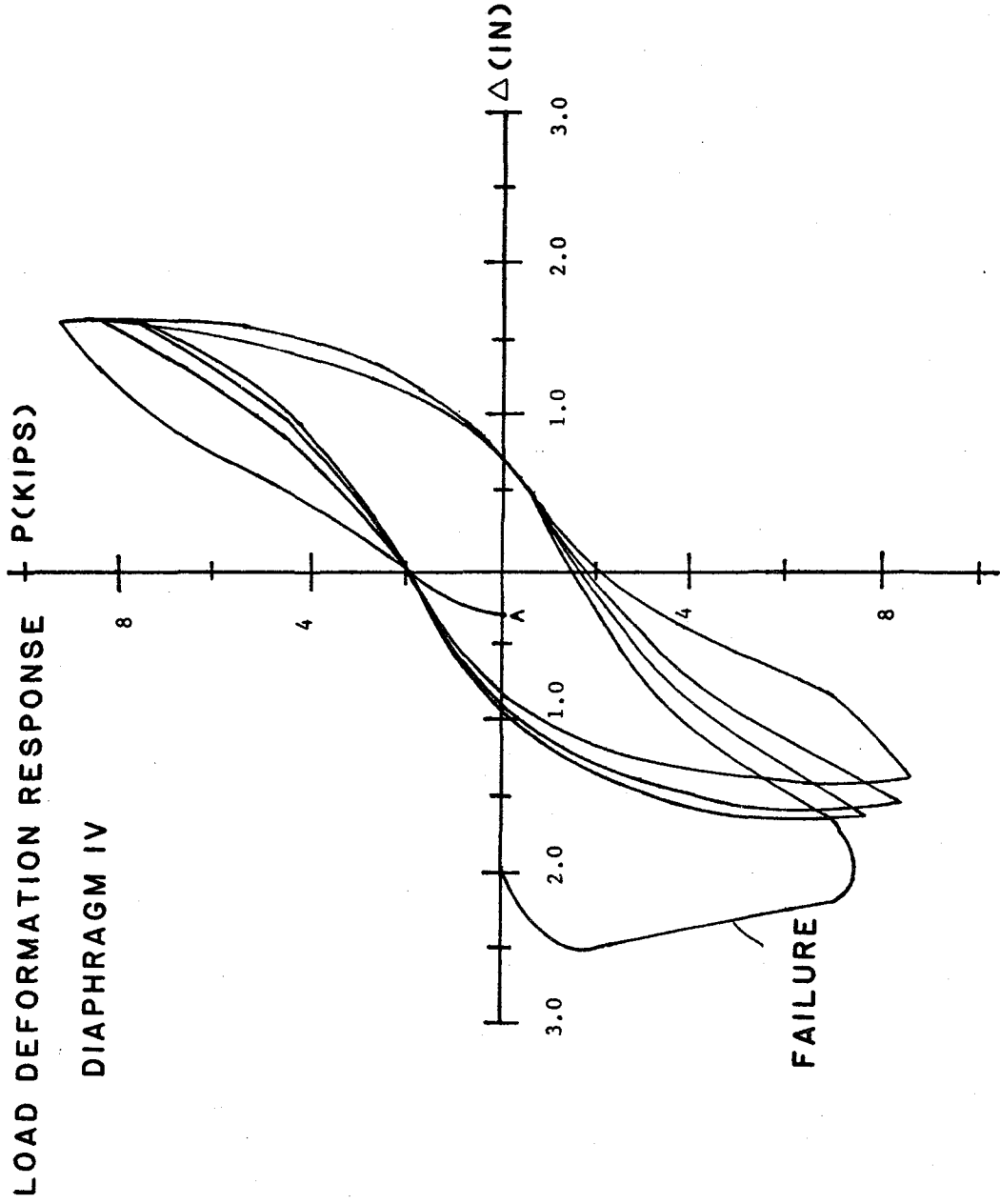


Figure 3-7. Load Shear Deformation Response of Diaphragm IV

deformations without experiencing significant shear degradation.

3.3 RIGID BODY DISPLACEMENTS

The in-plane, shear displacement behavior presented in Figs. 3.4 - 3.7, illustrates the general characteristics of diaphragm response. This behavior does not, however, provide a true quantitative measure of the response. The basic problem is that shear displacement data presented to this point include the contribution of support movement associated with the flexibility of the support components, as well as possible slack in the pin connections used as the experimental hinge supports.

The effect of support movement on diaphragm response was monitored during each test with dial gages positioned at both hinge positions to measure movement in the x and y directions (Fig. 2.7). On data reduction, the dial gage readings indicated two types of diaphragm rigid body motion; a translation in the direction of the applied load (Fig. 3.8a) and a rigid body rotation due to deformation normal to the load directions (Fig. 3.8b). Including the effect of support motion, the net displacement at position A (Fig. 2.7) due to diaphragm deformation may be expressed as:

$$\Delta_d = \Delta_s - \Delta_r - \Delta_t \quad (3.1)$$

where:

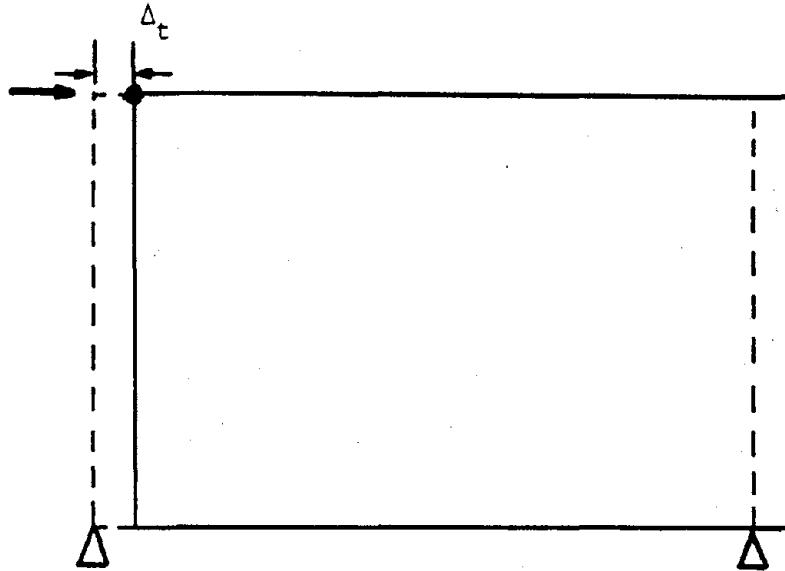
Δ_d = net displacement due to diaphragm deformation

Δ_s = experimentally measured diaphragm displacement

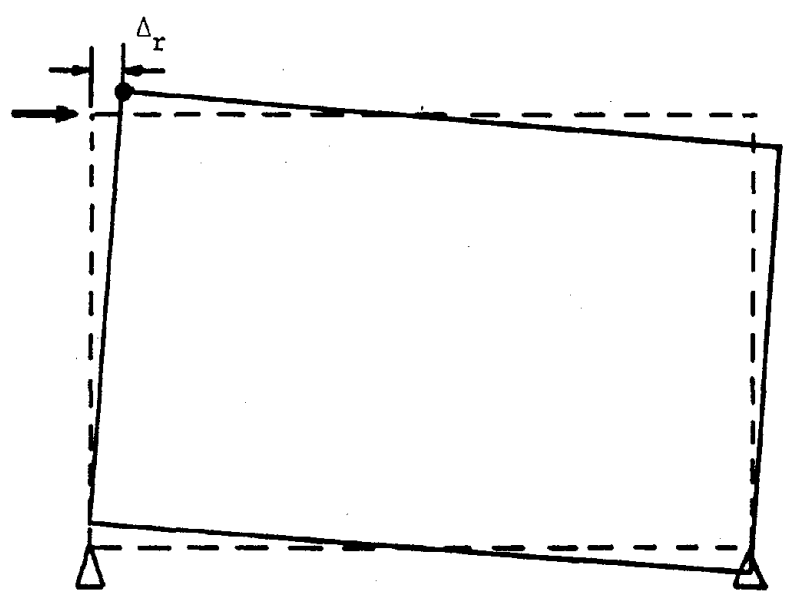
Δ_r = displacement due to rigid body rotation

Δ_t = displacement due to translation.

The measured values of Δ_r and Δ_t indicate that support movement has a significant effect on measured diaphragm displacement. For example, rigid body displacements in a typical test series II diaphragm accounted for approximately 50 percent of the measured displacement at 2 kips and 25 percent at 8 kips. The larger rigid body effect at 2 kips indicates that some



(a) Translation



(b) Rigid Body Rotation

- ➔ Applied Load
- Position of Diaphragm Displacement Readings

Figure 3.8. Rigid Body Displacements

slack may have existed in the pin connections.

Unless noted otherwise, reference to diaphragm response in the following discussion implies shear-displacement data corrected for rigid body displacements.

3.4 EFFECT OF DIAPHRAGM CONDITIONS ON RESPONSE

One aspect of the experimental investigation was to examine the influence of various design conditions on the response of timber diaphragms. In the following subsections, the effect on response of three factors considered in this investigation are summarized. The factors discussed are blocking arrangement, diaphragm openings, and plywood thickness.

3.4.1 BLOCKING

As discussed in Chapter 2, a basic change in diaphragm construction was made in Test Series II in that blocking, i.e., members running between and perpendicular to joists, was placed along plywood panel boundaries instead of at an arbitrary spacing of 5 feet-4 inches as in Series I. The reason for the change was to improve the nail slip response characteristics of panel joints perpendicular to the joists by allowing the nail spacing smaller than the joist spacing.

The effect of this change in the diaphragm blocking detail on the in-plane shear response is illustrated in Fig. 3.9. This figure compares the response of a typical diaphragm from Test Series I with the response of diaphragm II from Test Series II. The perimeter nail spacing and nail spacing parallel to the joists is 4 in. for the diaphragm from Test Series I, which is referred to as the unblocked diaphragm. A nail spacing of 6 in. was used for all plywood joints in the Test Series II diaphragm, referred to as the blocked diaphragm. The comparison of diaphragm response in Fig. 3.9 demonstrates that using a 6-in nail spacing throughout the diaphragm results in a significant improvement in diaphragm response. For example, the deflection at the

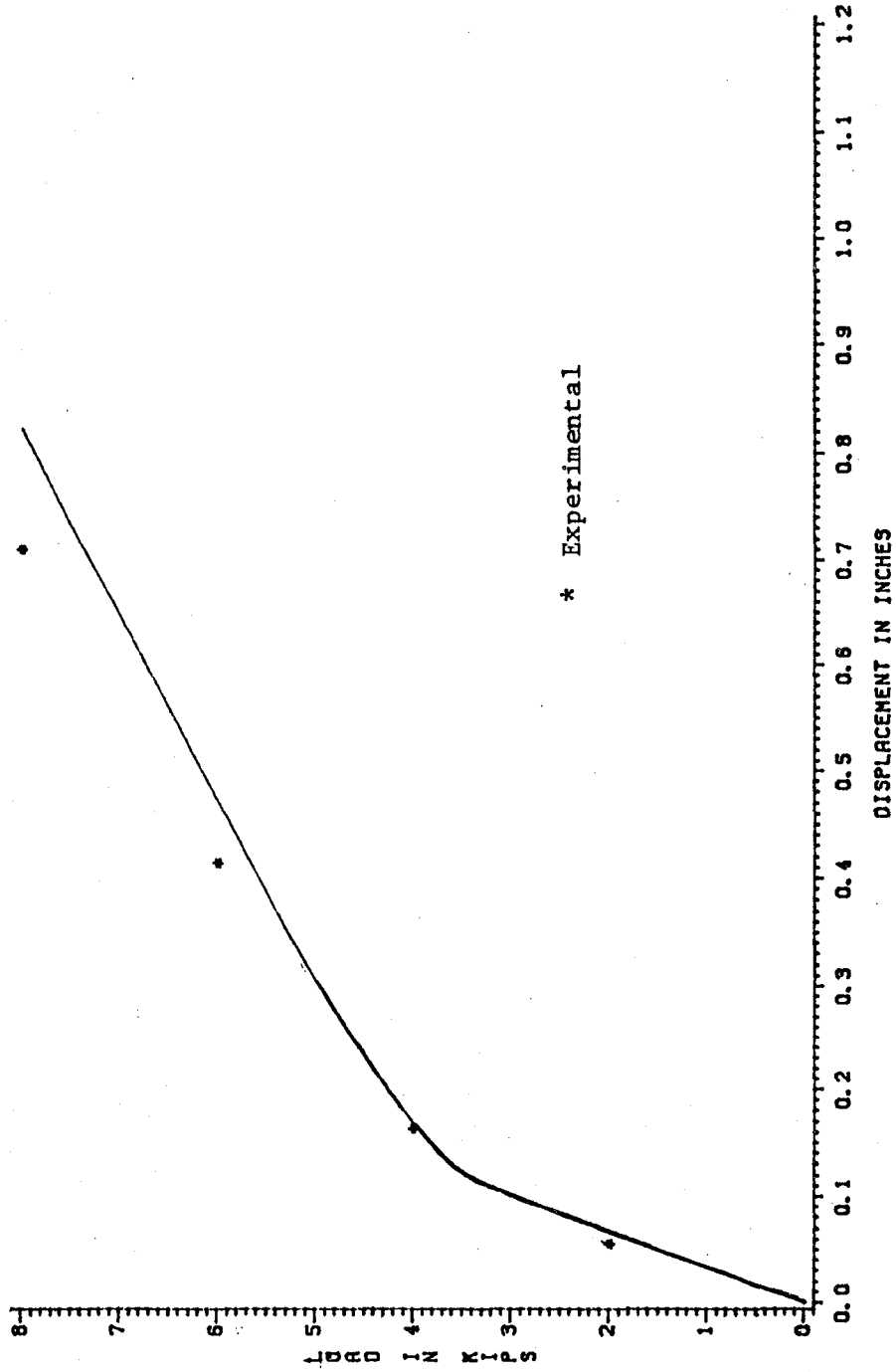


Fig. 3.9. Displacement of Blocked Diaphragm

maximum load of seven kips in the unlocked diaphragm was 1.12 in., while the value at the same load level in the blocked diaphragm was 0.56 in. In addition, the maximum load before a significant reduction in shear-displacement stiffness occurs increases from 7 kips in the unblocked diaphragm to 10 kips (Fig. 3.4) in the blocked diaphragm.

3.4.2 CORNER OPENING

Diaphragms with corner openings (Fig. 2.5) were tested in both experimental series. The behavior of the diaphragm with an opening in Test Series I indicated a serious shear transfer problem existed at the opening. This problem resulted in a significant reduction in strength and stiffness when compared to a diaphragm without an opening (6).

Recently, the ATC (21) recommended design details to improve the shear transfer characteristics at openings in timber diaphragms. Diaphragm III of Test Series II was constructed with an opening detailed following the ATC recommendations in order to evaluate the effectiveness of these opening details.

A comparison of the shear-displacement response for diaphragm II (Fig. 3.5) and III (Fig. 3.6), which were the same except for the opening in diaphragm III, indicates that although the opening causes a decrease in strength* from 10 kips to 8 kips, the general response characteristics are similar. In addition, model failure in both diaphragms was attributed to closure board rotation.

In view of the response of diaphragm III, it appears that the design details recommended by ATC provide an effective means of shear transfer at openings.

*Load at which the shear displacement stiffness approaches zero.

3.4.3 PLYWOOD THICKNESS

The effect of plywood panel thickness on in-plane shear behavior was examined in test series II by changing the typical panel thickness in diaphragm V from 1/2 to 3/4-in. A comparison of the shear displacement response of diaphragm IV (Fig. 3.4) and V (Fig. 3.10)**, which were the same except for plywood thickness, indicates that cyclic shear degradation begins at a lower load level in diaphragm V with 3/4 in. plywood than in diaphragm IV with 1/2 in. plywood. For example, shear degradation as a result of load cycles at six kips in diaphragm IV stabilized after the first cycle. In diaphragm V, however, the shear degradation continued with each cycle, indicating some cyclic degradation of the nail-slip mechanism between panels. This apparent detrimental effect on response of increasing plywood thickness is attributed to the fact that, since the same nail size was used in the panel connections for both thicknesses, the thicker plywood reduced nail penetration into the connecting member, thus reducing the effectiveness of the nail-slip effect.

3.5 SUMMARY OF RESULTS FOR TEST SERIES I

The test series are designed to evaluate the diaphragm behavior under static and dynamic loads for varying problem parameters. The relative movements and stiffness variations under different loads are recorded and synthesized. For example, in-plane stiffness of a plywood sheet is considerably greater than the stiffness of the same size unit put together using smaller units and nailed joints. Therefore, measurements are limited to the movements of one piece of material with respect to another and not within a plywood sheathing. In addition, out-of-plane movements of small magnitudes are observed. These movements develop, perhaps, due to torsional moments caused by warping in the diaphragm itself.

**The displacement data in these figures have not been corrected for rigid body displacements.

The corner distress at higher loads, in terms of separations and rotations, is highly visible in these experiments. This is due to high stress concentration effects at re-entrant angles. The corner nails can offer little resistance to separation, where both sides of a corner are fixed. In addition, the closure board-sill plate, and closure board-deck attachments seem to act differently for different load directions. A second type of corner test (one side fixed and the other free) reveals that it is highly flexible, and the load carrying capacity is only 1/5 of that of a case with fixity of both sides of a corner. Even additional stiffening of the corner did not significantly increase the overall diaphragm stiffness. In general, the overall behavior of a diaphragm appears to have been critically affected by corner conditions either for rectangular diaphragms or those at the interior of the structural system, such as cases having openings in the diaphragm system.

Plywood sheets, when staggered at joints, act in groups and tend to expand outward as more rows of sheets are added. Hence the work done by diaphragms does not directly depend on the diaphragm area, but it is a function of the number of smaller units that are working together in resisting the in-plane forces, (refer to Fig. 4-5 and 4-6 and Pages 45-46 of reference 6). Diaphragms with staggered joints are found to be as much as 15 percent stiffer than those with aligned joints.

Use of the slanted nailing, or tow-nailing between the sheathing and joists showed some increased sliding or slip along the joints. However, their resistance is nearly equal to that of nails applied perpendicular to the diaphragm surface. When nails are used near the edge of plywood sheathing, they exhibited lower load-slip capacity under the application of load perpendicular to the surface grain as opposed to the load acting parallel to the grain. For a given amount of slip, a joint parallel to an applied loading sustains about 20 to 50 percent more load than a joint with perpendicular loading. After initial slip, a nail joint that is subjected to repeated loads

exhibited no loss of stiffness up to a certain magnitude of loading. An increase in slip is found only for larger loads; however, overall integrity of a joint is still maintained for all practical purposes.

Short-term static loads seem to result in maximum stiffness for the structure whereas repetitive loadings tend to reduce the stiffness. During the application of dynamic sinusoidal loads, 95 percent of the displacement appears to take place in the first 500 cycles of loading, and also 25 to 75 percent of that displacement occurs at the initial application of the load. Damping for those diaphragms that were tested under this research program varied between 1.35 and 6.22 percent of critical damping. It appears that diaphragms with 6-in. nail spacing provided greater damping than those with 4-in. nail spacing. This simply is due to the greater shear-slip movement for the former case.

Joist hangers result in simple joint attachments, but they do tend to make a diaphragm more flexible. The diaphragms with such hangers are 18 and 26 percent more flexible (than the one with directly nailed joists), in the positive and negative loading zones, respectively. Also, the slip is about 28 percent greater in structures with hangers. Hence, for design purposes, different stiffness and slip factors must be assigned depending on joint and attachments.

4. ANALYTICAL MODEL AND RESULTS

A finite element model formulated to predict the in-plane shear response of timber diaphragms is described in this chapter. After discussing the basic characteristics of the model, the results of two analytical studies carried out as part of the investigation are presented. In the first study, the effects of plywood material properties and nail-slip stiffness on diaphragm response are quantified. In the second study, analytical response is compared to observed experimental response.

4.1 FINITE ELEMENT MODEL

In the finite element method of structural analysis, a structure is idealized as a series of elements for which the state of interest (for example, structure state of stress) is expressed in terms of a selected set of discrete parameters. On the basis of the relationship between these parameters and the desired element state, and the connectivity between the various elements used to idealize the original structure, a set of linear* equations are formulated with the discrete parameters as unknowns. Solving these equations for the discrete parameters, the desired structure state may be determined by evaluating the various element states.

For example, consider a typical plywood panel in a timber diaphragm. The panel behavior is of concern in predicting diaphragm response to in-plane shear forces and the shear force-deformation response. The panel characteristic may be modeled using finite elements which relate the state of stress caused by in-plane shear forces to a set of discrete nodal displacements.

A number of such elements exist, and the one used in a given problem depends on the state of stress which is being idealized. The nature of the

*It is assumed that the relationship between the discrete element parameters and the element state is linear.

panel loading (in-plane shear) in conjunction with the small panel thickness, lead to the conclusion that a finite element which models a plane stress condition should adequately represent the panel stress state.

The choice of a plane stress element is advantageous from a computational point of view since the resulting two-dimensional problem will require fewer unknown nodal displacements to adequately define the panel state of stress. Consequently, the computational effort required to solve the resulting set of linear equations is reduced. In addition, evaluation of element properties for two-dimensional elements typically involves less computation than that required for evaluation of three-dimensional element properties.

Once a finite element model for a typical plywood panel is selected, a model for the diaphragm may be obtained by repeating this idealization for each panel in the diaphragm and coupling nodal displacements common to the adjacent panels. This coupling process presents a problem in the case of plywood shear diaphragms in that relative motion between panels is possible due to nail slip. This apparent difficulty is overcome by connecting panels with dimensionless link elements with stiffness characteristics defined to represent nail-slip response.

Additional details of the finite element model considered in this investigation are discussed in the following sections.

4.1.1 PLYWOOD PANEL IDEALIZATION

A typical plywood panel is idealized as a substructure of four-noded isoparametric quadrilaterals (Q4 element). This particular element was chosen to simplify panel mesh stiffness computation, as well as simplify the problem of defining the connectivity between plywood panels. Although wood is in general an orthotropic material, the orientation of the grain in the various plies through the thickness of a plywood panel results in a material which is essentially isotropic. As a result, an isotropic plane stress constitutive

relationship is considered in computing Q4 element stiffness properties.

For the mesh size defined by the user, the panel substructure stiffness is formed and then condensed to a new stiffness relating panel boundary forces to boundary displacements (20). This stiffness formation and condensation is repeated only for each different panel in the diaphragm. Since the diaphragms considered in this study involved only two different panels (Figure 2.4), only two panel stiffness formations and condensations were required.

The substructure approach used in this investigation is very efficient computationally for structures in which similar components (in this case plywood panels) are repeated a number of times. Study of the effect of panel mesh size, however, indicates that panel response is adequately modelled by a relatively coarse mesh (20). Consequently, substructuring may not be the best approach in this particular problem.

4.1.2 NAIL SLIP IDEALIZATION

The results of previous investigations, as well as the results of the experimental phase of this investigation, indicate that the shear transfer from panel to panel via fasteners (typically nails) and intermediate framing elements (joists) is a major factor influencing diaphragm in-plane shear response. To incorporate this factor into the model, different nodal points are specified at the same global coordinates corresponding to the positions of joints between panels. Adjacent panels are then connected by dimensionless links with stiffness properties that represent the nail-slip response for both in-plane directions. Consequently, relative movement between adjacent panels is possible.

A typical link element consists of two orthogonal springs (Fig. 4.1) in which the nail stiffness in the x direction is K_x , the nail stiffness in the y direction is K_y , and the arrows represent the directions of the local degrees of freedom (DOF). In the current model, the values of K_x and K_y are assumed

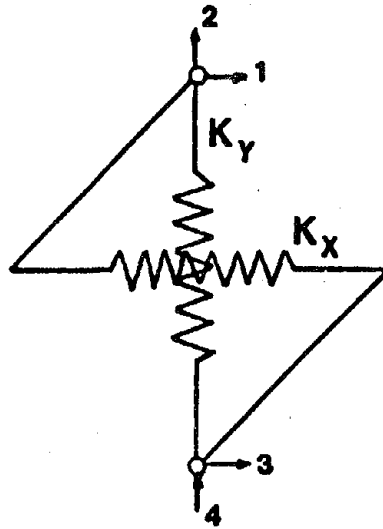


Fig. 4.1. Link Element

equal.

Due to the relative importance of nail slip to overall diaphragm response, a reasonably accurate idealization of nail slip stiffness was desired. In particular, modeling the nonlinear aspect of nail-slip response was considered important. In the view of this concern, the bilinear nail slip relationship (Fig. 4.2) suggested by GangaRao and Luttrell (9) in the initial stage of this investigation is employed to define the basic nail-slip stiffness considered in the model. A modification of this bilinear stiffness relationship based on the nail slip response proposed by the American Plywood Association (22) was also considered in the analyses conducted as part of this study.

The stiffness assigned to a given link is the net stiffness of the group of nails assumed tributary to that link. Considering force equilibrium and displacement compatibility, the total nail stiffness, K , between two panels may be shown to be (20)

$$K = \left(\frac{N_1 N_2}{N_1 + N_2} \right) SN \quad (4.1)$$

where:

N_1 - is the total number of nails along panel 1.

N_2 - is the total number of nails along panel 2.

SN - is the stiffness corresponding to one nail.

The total stiffness K , is distributed to the links between two panels on the basis of the lengths between adjacent links (20).

4.1.3 FORMATION OF DIAPHRAGM STIFFNESS

Once the panel stiffness matrices are defined, they are assembled to define the diaphragm stiffness. This is essentially a bookkeeping problem in which panel stiffness terms are placed into the global stiffness matrix, and all nodes with common global coordinates are connected using the dimensionless link elements.

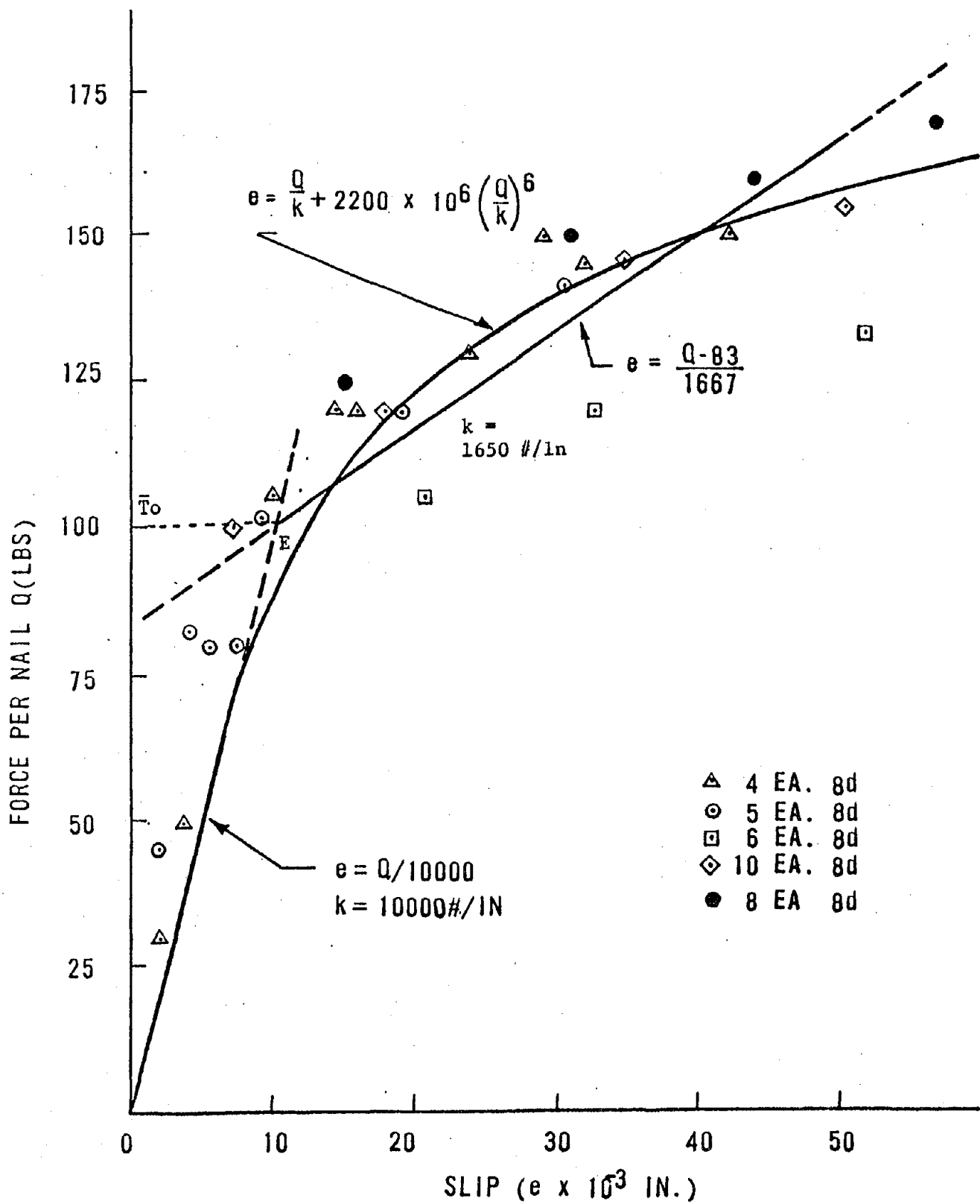


Fig. 4.2. Slip Factors for 8d Nails in $\frac{1}{2}$ " Plywood

Storage requirements for the global stiffness matrix are reduced by recognizing symmetry. In addition, only the values within the stiffness profile defined by the uppermost nonzero location for each column of the global stiffness matrix are stored.

4.1.4 BOUNDARY CONDITIONS

A typical cross section of the diaphragm boundary is shown in Fig. 2.3. The steel load frame shown in this diagram is included in the model formulation so that the load applied to the analytical floor diaphragm model would be the same as that applied experimentally (Fig. 2.1). In addition, including the steel load frame makes it possible to include the slip between the load frame and floor diaphragm in the analytical model.

The load frame is modeled as a series of truss elements. To incorporate the truss elements into the model, additional nodes are defined around the perimeter of the diaphragm, and are connected to the diaphragm with dimensionless links representing the slip stiffness between the load frame and floor diaphragm.

Examination of the details used in connecting the experimental diaphragm to the steel test frame (Fig. 2.3) indicates three possible slip mechanisms: slip between the sill plate and steel frame, between the closure board and sill plate, and between the plywood panel and closure board. On the basis of observed experimental response, the slip between the plywood panel and closure board is considered significantly more flexible than the other mechanisms. As a result, the dimensionless link stiffness for the links connecting the floor diaphragm to the boundary frame correspond to the plywood panel, closure board slip mechanism.

4.1.5 PANEL BEARING

The movement of plywood panels on load application is shown in Fig. 3.5. It is evident on examination of this response that some panels bear against

each other. As presented so far, the analytical model is unable to account for panel bearing, and an analysis would indicate that panels overlap. To avoid this overlapping problem, an arbitrary load is applied to the diaphragm, and nodal displacements are found by solving the equilibrium equations:

$$\underline{K}_i \underline{U}_i = \underline{R}_a \quad (4.2)$$

where:

\underline{K}_i = initial diaphragm stiffness matrix

\underline{U}_i = initial nodal displacement vector

\underline{R}_a = applied load vector

The initial stiffness matrix is then modified by identifying all overlapping nodes, and assigning high stiffness (1×10^7 k/in. compared to a typical link stiffness of 1×10^4 k/in.) to the links corresponding to the overlapping DOF. This change constrains the DOF perpendicular to the overlapping boundaries to move together on load application. The solution process is then restarted based on the new stiffness matrix.

4.1.6 NONLINEAR SOLUTION OF EQUILIBRIUM EQUATIONS

As a result of the bilinear nail-slip idealization, a nonlinear solution scheme is required to determine the response of a diaphragm using the proposed model. The solution scheme considered in this study is illustrated in Fig. 4.3. In a typical solution step, a load increment of X force units is applied to the diaphragm, where X can be any value less than or equal to the total load to be applied to the diaphragm. The resulting increment of diaphragm displacements is then found by solving the equilibrium equations:

$$\underline{K}_t \underline{U}_{inc} = \underline{R}_{inc} \quad (4.3)$$

where:

\underline{K}_t = diaphragm stiffness matrix modified to reflect the reduced stiffness of all links in region S2 of the nail slip relationship (Fig.4.4a), referred to as the current tangent stiffness.

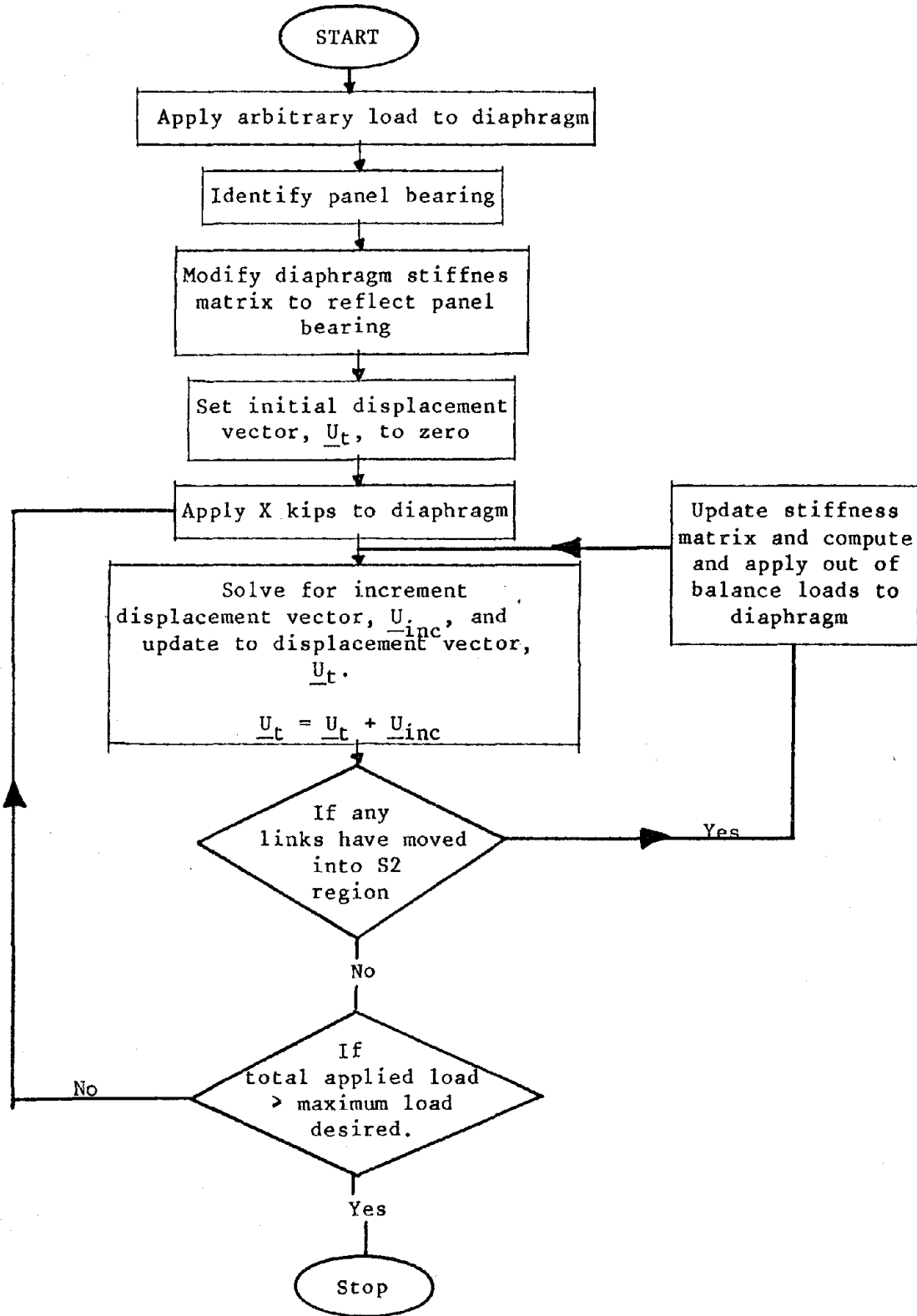


Figure 4.3 Flow Chart of Solution Scheme

\underline{U}_{inc} = incremental displacement vector.

\underline{R}_{inc} = incremental load vector.

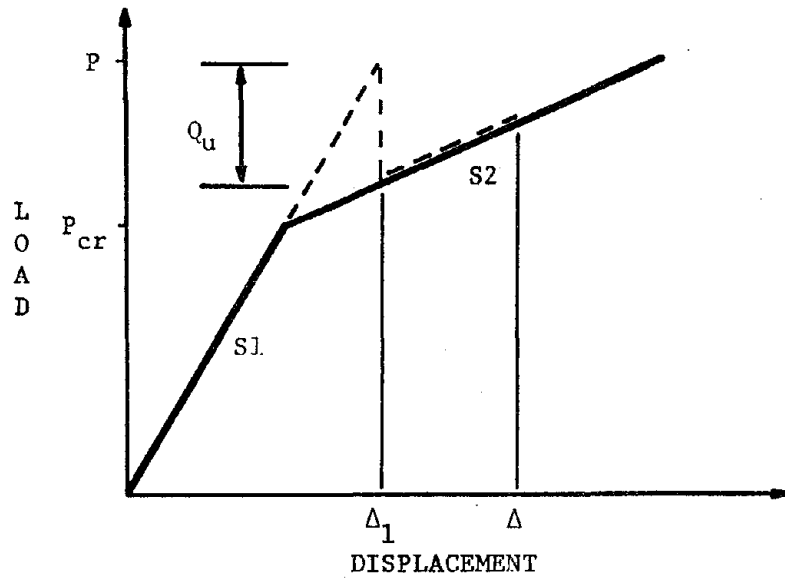
At this point, the nail slips are evaluated based on the total displacement vector, which is the sum of all previously calculated displacement vectors, and all links for which the slip is in region S2 of Fig. 4.4a are identified. Out of balance nodal loads exist (Q_u), at these links, because the nodal loads corresponding to the current displacements are based on the S1 stiffness, whereas the nodal loads are actually a function of S1 and S2 (Fig. 4.4a). Consequently, before the next load increment is applied, a sequence of equilibrium correcting iterations are carried out to eliminate this equilibrium violation.

In a typical iteration, the incremental displacements corresponding to the unbalanced nodal loads \underline{R}_b are evaluated by solving the equations:

$$\underline{K}_t \underline{U}_{inc} = \underline{R}_b \quad (4.4)$$

Once \underline{U}_{inc} is known, the total displacement vector \underline{U}_t is updated, and new link slips are computed. If additional links reach S2, the basic iteration cycle is repeated. If S2 is not reached, the total load on the diaphragm is compared to the total desired load. If the total desired load has been reached (or exceeded), the solution process is stopped, otherwise the next load increment is applied and the solution process is repeated.

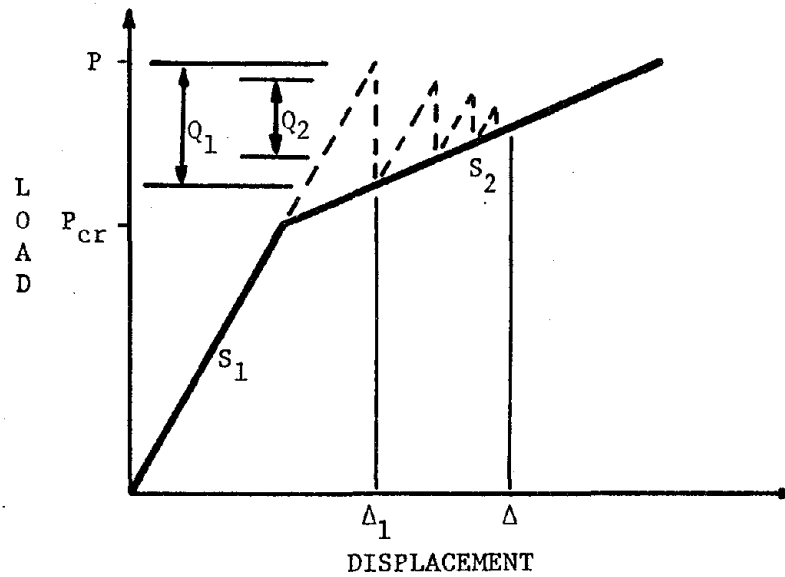
The tangent stiffness technique discussed above has the disadvantage of requiring many time-consuming stiffness triangularizations. In an attempt to avoid this, a constant stiffness iteration scheme was examined. In this technique, the stiffness matrix remains constant after it has been modified to account for panel bearing. Consequently, only two stiffness triangularizations are required. For each load increment, equilibrium correcting iterations are required, similar to those discussed above for the tangent stiffness scheme.



S1 = Nail Stiffness Below P_{cr}

S2 = Nail Stiffness Above P_{cr}

(a) Tangent Stiffness Scheme



Q_1 = First Out of Balance Load

Q_2 = Second Out of Balance Load

(b) Constant Stiffness Scheme

Figure 4.4 Nonlinear Solution Schemes

The basic features of the constant stiffness scheme is shown in Fig. 4.4b. On comparing the two solution schemes, it was concluded that the advantage of requiring only two stiffness triangularizations in the constant stiffness scheme is outweighed by the increased number of equilibrium iterations required at each load level. Consequently, the tangent stiffness scheme has been used in all analyses presented in this report.

4.1.7 MODEL LIMITATIONS

A limitation on panel geometry exists in the current model. Basically, the dimensions of a typical panel Q4 element must be the same for all panel substructures. This limitation exists to ensure that boundary nodes of adjacent panels have common global coordinates.

As a result of this limitation, the model is limited to panels in which the dimensions correspond to integer multiples of the typical plywood sheet used in constructing the diaphragm. Consequently, it is not possible to analyze the experimental diaphragms considered in this study with openings.

A second limitation corresponds to the type of loading. The model, as currently formulated, is limited to monotonic in-plane shear loading.

4.2 PARAMETER STUDY RESULTS

There are four basic material properties involved in the proposed diaphragm model: Young's modulus (E), Poisson's ratio (V), and thickness (TH) of the plywood panels; and the stiffnesses, S1 and S2, used to define the bilinear nail-slip relationship (Fig. 4.4). To evaluate the effect of these parameters on diaphragm response, a set of analyses were carried out in which each material parameter is independently increased and decreased by a factor of 2 from an assigned reference value. The reference values considered are:

$$E = 1 \times 10^6 \text{ k/in}^2$$

$$V = 0.236$$

TH = 0.5 in

S1 = 10,000 k/in

S2 = 1,667 k/in

The value for E is that given in Reference 23 for 1/2-in. plywood type group 3. The value of V is the average for Douglas Fir parallel and perpendicular to the grain listed in Reference 24. The nail slip stiffnesses are based on the relationship proposed by GangaRao and Luttrell (Fig. 4.2).

The effects on model response of variations in the plywood material properties are summarized in Tables 4.1-4.3. Changes in Poisson's ratio have a very minor effect on response, altering the diaphragm displacement results by less than 1 percent (Table 4.1). Young's modulus and plywood thickness have only a slightly more significant effect (Tables 4.2 and 4.3). Increasing either of these parameters by a factor of 2, decreases displacement by about 4 percent, while decreasing them by the same factor, increases diaphragm displacement by about 7 percent.

The effect on model response of changing the values of link stiffnesses S1 and S2 are shown in Fig. 4.5. Increasing both S1 and S2 by a factor of 2, reduces diaphragm displacement by a factor of 4 at the peak loading of 8 kips, while decreasing both S1 and S2, increases diaphragm displacement by a factor of 2.5 at this load. In addition to the significant changes in diaphragm displacement caused by changes in link stiffness, the relative importance of link stiffness on response is illustrated by the fact that the force displacement relationship has the same shape as the link stiffness relationship (Fig. 4.5).

In view of the analytical results summarized in Tables 4.1 through 4.3 and Fig. 4.5, it is apparent that nail slip stiffness is by far the most significant parameter influencing diaphragm response.

It should be noted that, in evaluating the effect of plywood thickness, the influence of the change in thickness on nail-slip response was not considered.

Table 4.1 Effect of Poisson's Ratio on
Diaphragm Displacement (in inches)

Load (kips)	Poisson's Ratio (ν)		
	$\nu = 0.118$	$\nu = 0.236$	$\nu = 0.472$
2	0.060	0.061	0.062
4	0.146	0.147	0.149
6	0.416	0.418	0.422
8	0.721	0.724	0.729

Table 4.2 Effect of Young's Modulus
on Diaphragm Displacement (in inches)

Load (kips)	Young's Modulus (E)		
	5×10^5 k/in ²	1×10^6 k/in ²	2×10^6 k/in ²
2	0.069	0.061	0.056
4	0.165	0.147	0.136
6	0.449	0.418	0.401
8	0.772	0.724	0.700

Table 4.3 Effect of Plywood Thickness
on Diaphragm Displacement (in inches)

Load (kips)	Plywood Thickness (inches)		
	0.25	0.5	1.0
2	0.069	0.061	0.056
4	0.165	0.147	0.136
6	0.449	0.418	0.401
8	0.772	0.724	0.700

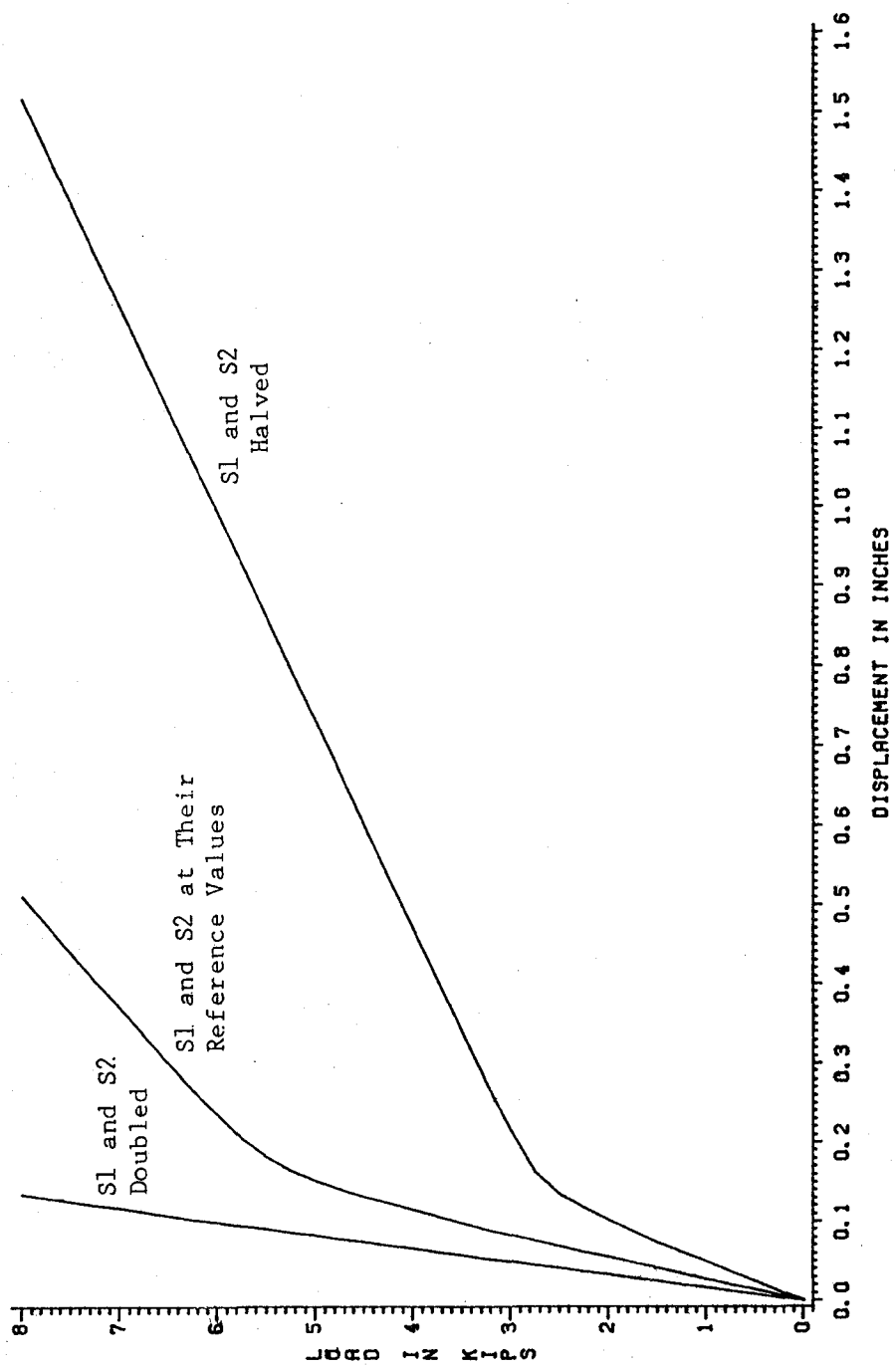


Figure 4.5 Effect of Changing S1 and S2 About Their Reference Values on Displacement of Blocked Diaphragm

On the basis of the experimental response observed when the plywood thickness was changed from 1/2 to 3/4 in. (section 3.3.2), it appears that nail-point penetration is important in terms of the response and also a coupling between nail-slip and plywood thickness exists. This coupling, however, is not reflected in the results presented in Table 4.3.

4.3 COMPARISON OF ANALYTICAL AND EXPERIMENTAL RESULTS

As a result of the limitations on panel geometry and model load history discussed in Section 4.1.7, a comparison of analytical and experimental results is possible for a limited number of diaphragms. In the following subsections, the analytical results for a diaphragm from each experimental series are discussed. Both diaphragms analyzed were 16 by 24 ft. The diaphragms differed in the blocking details employed and the nail spacing used in the panel joints. The blocking for the Series I diaphragm was spaced at 5 ft - 4 inches, its primary function being to brace the joists. In the following discussion, this diaphragm is referred to as the unblocked diaphragm.

A consequence of this blocking arrangement is that nail spacing along interior plywood panel boundaries perpendicular to the joists is equal to the joist spacing of 16 in. Nail spacing for panel joints around the perimeter of the diaphragm, as well as joints parallel to joists, was 4 in.

The blocking for the diaphragm analyzed from Test Series II (diaphragm II) was along lines corresponding to plywood panel joints. Consequently, it was possible to use the same nail spacing of six inches along interior panel joints perpendicular and parallel to the joists. In the following discussion, this diaphragm is referred to as the blocked diaphragm.

One factor concerning diaphragm construction which has not been addressed to this point is the effectiveness of nailed joints. The relatively narrow nailing surface provided along joists (as well as blocking) typically requires the use of toe nailing when making interior panel joints, i.e., the nails had to

(25) recommends using a toe-nail connection stiffness of five-sixths the straight nail stiffness for connections in ordinary wood. Similar recommendations for toe-nailed connections in plywood are not available, however.

In an attempt to bound the effect of nailed joint effectiveness, two analyses have been carried out for each diaphragm. In one analysis, referred to in the following discussion as the lower bound analysis, the nominal straight nail stiffness is considered. In the second analysis, referred to as the upper bound analysis, two-thirds of the straight nail stiffness is considered. It should be noted that for the unblocked diaphragm, the reduction in nail stiffness in the upper bound analysis is considered only along joints parallel to joists, since toe nailing was not required for joints perpendicular to joists.

All slip and displacement responses referred to in the following discussion correspond to positions of experimentally measured data shown in Fig. 2.8. In the discussion, the experimental diaphragm displacement response has been corrected to eliminate rigid body displacements. In addition, nail slip stiffness model 1 refers to the relationship proposed by GangaRao and Luttrell (9), and model 2 refers to the relationship based on the American Plywood Association data (22).

4.3.1 UNBLOCKED DIAPHRAGMS

A comparison of the experimental unblocked diaphragm response with the upper and lower bound analysis results found by considering link stiffness model 1, is shown in Fig. 4.6. In addition, upper bound results found considering link stiffness model 2 are given. A comparison of the results for link stiffness models 1 and 2 indicates that the two models predict essentially the same response after the transition in force displacement stiffness at a load level of approximately two kips. In the initial load range, the nail slip stiffness based on the American Plywood Association (22) data results in a

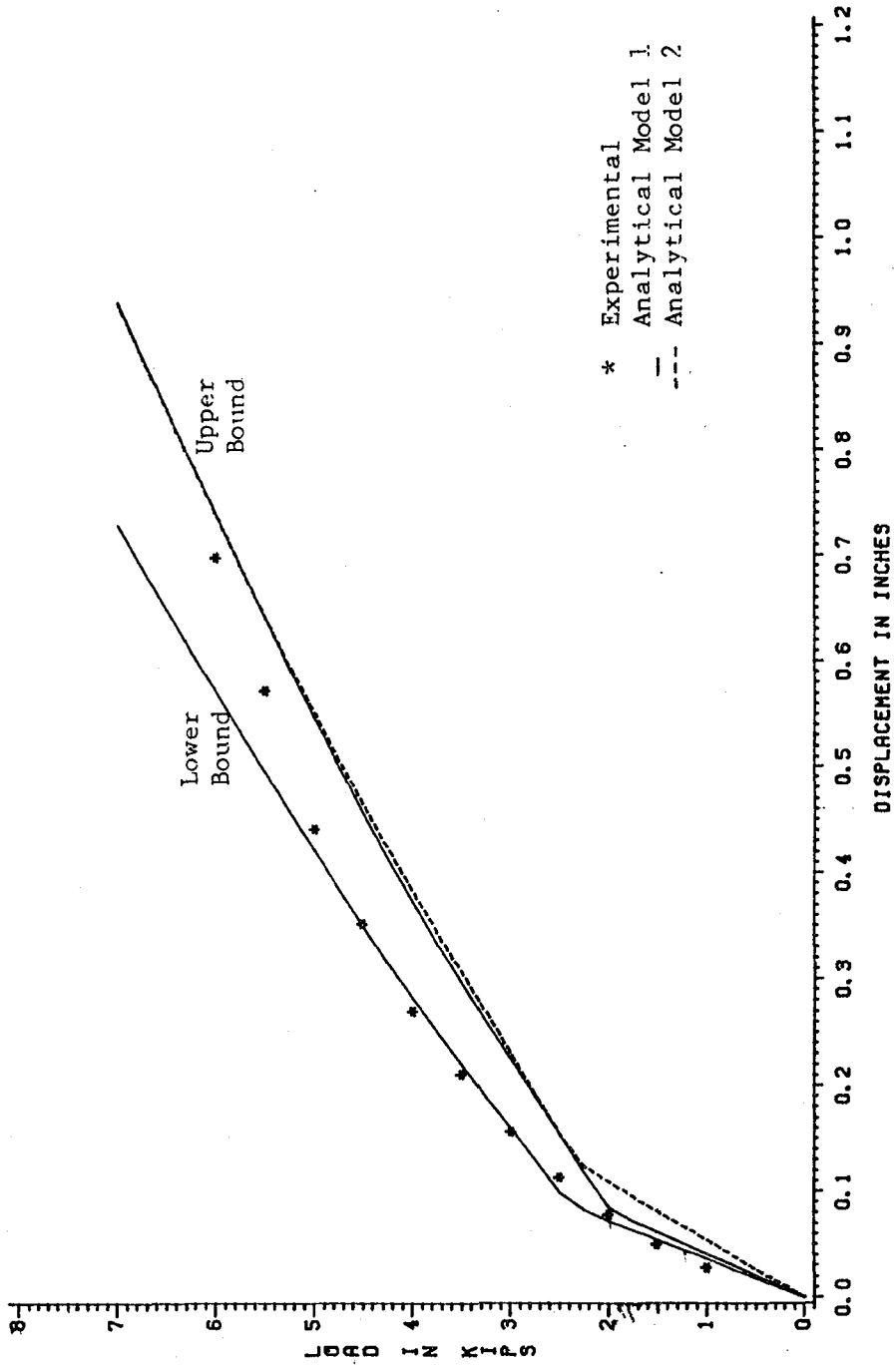


Figure 4.6 Displacement of Unblocked Diaphragm

more flexible response than that proposed by GangaRao and Luttrell (9).

A comparison of the experimental and analytical results in Fig. 4.6 indicates that the lower bound analysis closely predicts the response up to a load of approximately 5 kips. At larger loads, however, the experimental response is more flexible than the predicted response. This result indicates that the bilinear nail slip relationship considered in this study does not adequately reflect the apparent degradation in nail slip stiffness which occurs at high load levels.

The relatively good prediction of experimental results found by the lower bound analysis indicates that the effect of toe nailing on response in the unblocked diaphragm is relatively small. This observation is attributed to the fact that the unblocked diaphragm response is controlled primarily by panel joints perpendicular to the joists which, due a relatively large nail spacing (16 vs 4 in.), are more flexible than joints parallel to the joists. Since the joints perpendicular to the joists were straight nailed, toe nailing should have little effect on overall response.

Nail-slip results corresponding to the model 1 and model 2 analysis are compared to experimental slip data in Figs. 4.7-4.9. As indicated in Fig. 4.7 the data found considering nail slip stiffness models 1 and 2 are essentially the same. Consequently, only the slip data corresponding to model 1 are given in subsequent figures.

On comparing the analytical and experimental slip data, it is apparent that the analytical model correctly identifies which panel slips are large and those that are small. The significant difference in magnitude for the various panel slips is attributed to the panel bearing effects illustrated in Fig. 3.4. Panels tend to slide in groups, such as panels P1, P5, P6, P10, and P11, in response to in-plane shear. As a result, the slips at positions 1 and 5, (Figs. 4.7 and 4.8), which are between panel groups, are large relative to the slip at position 7 (Fig. 4.9), which is within a panel group.

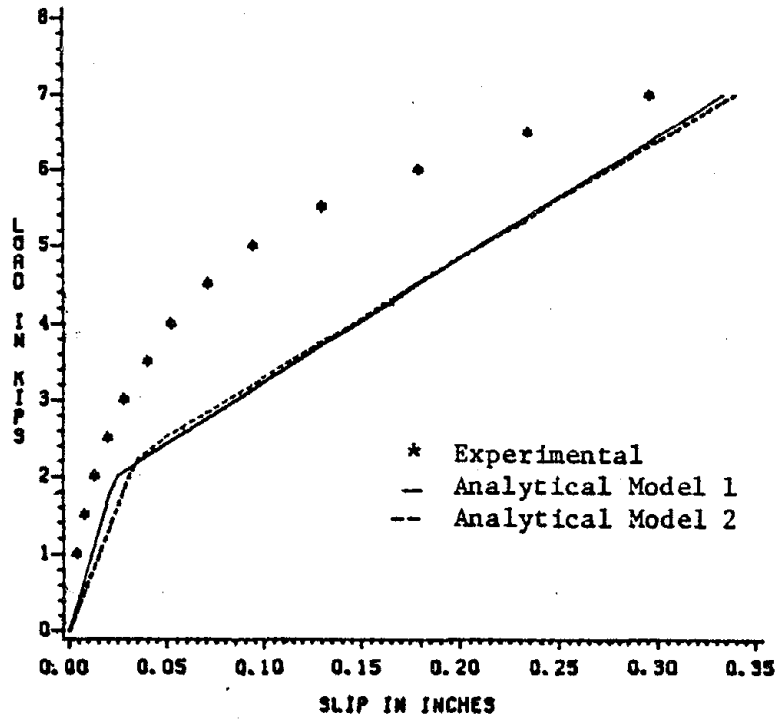


Fig. 4.7. Slip at Position 1 of Unblocked Diaphragm

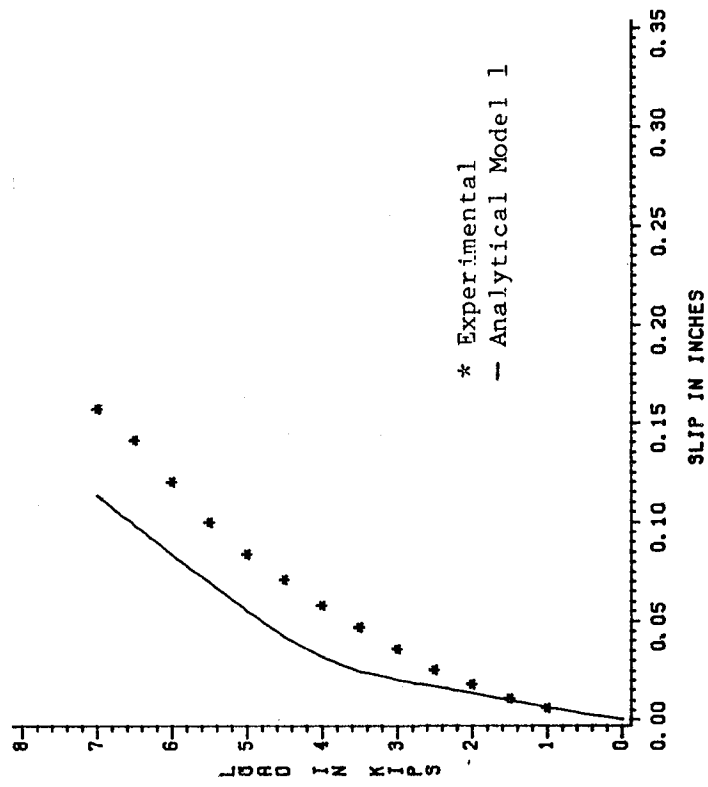


Figure 4.9 Slip at Position 7 of Unblocked Diaphragm

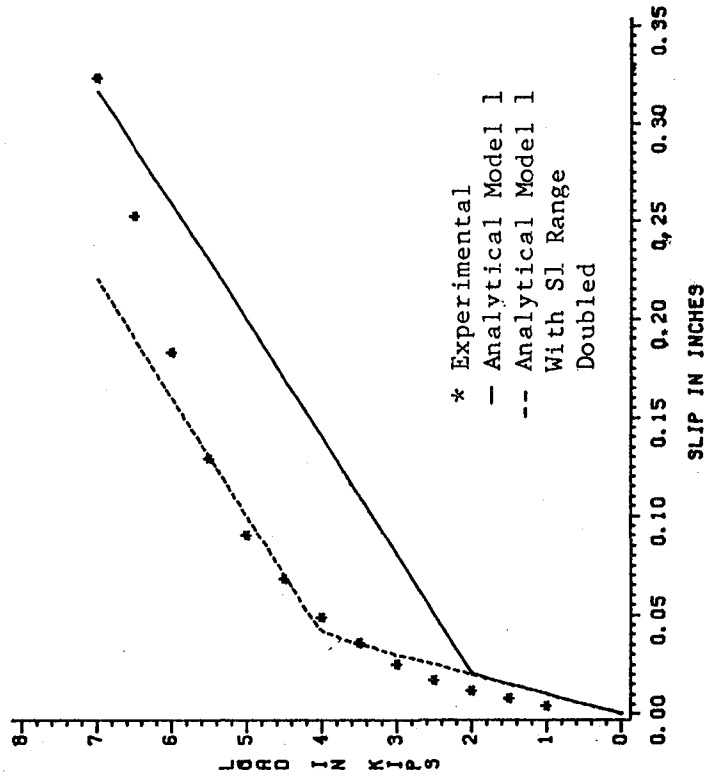


Figure 4.8 Slip at Position 5 of Unblocked Diaphragm

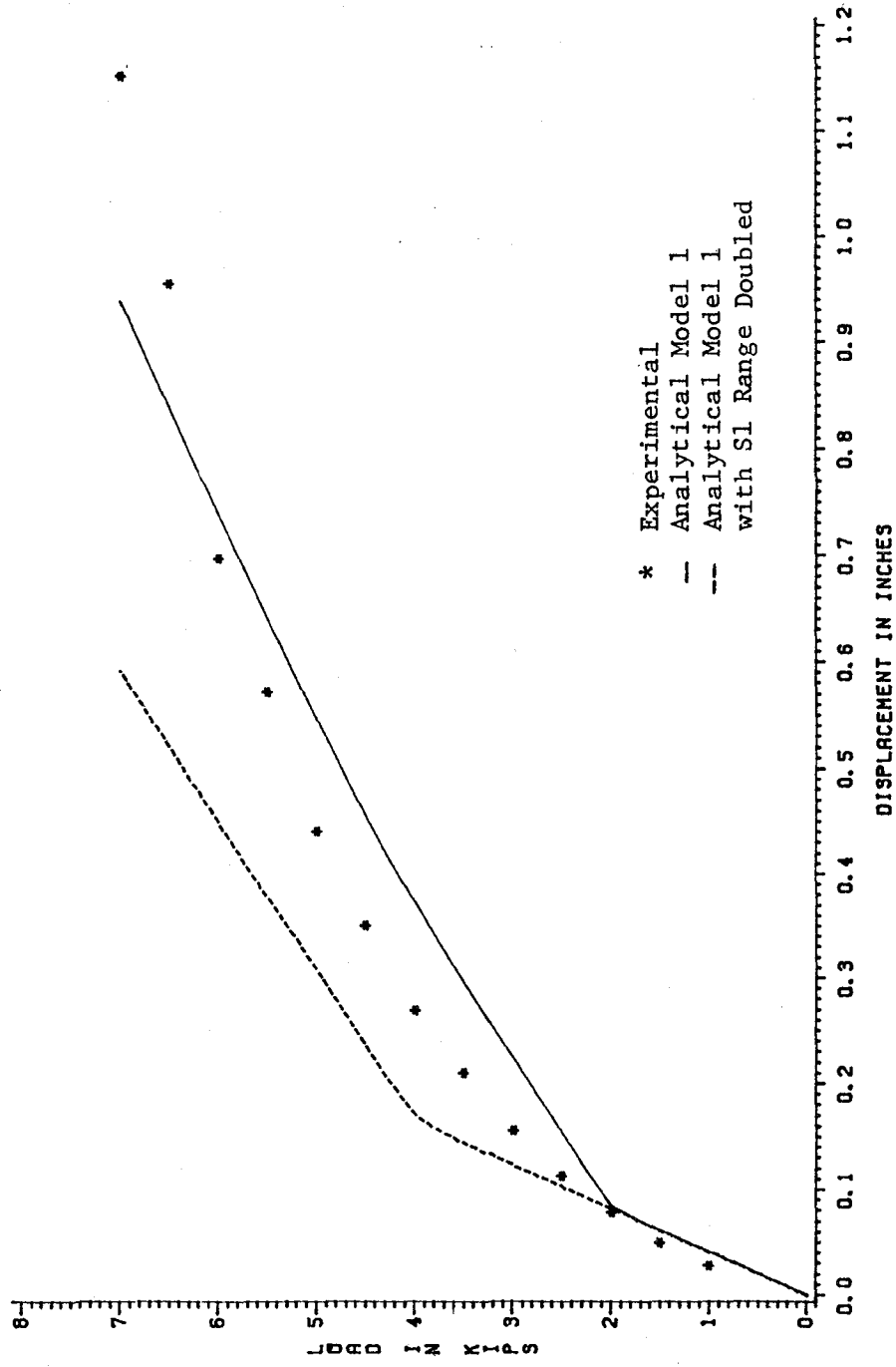


Figure 4.10 Displacement of Unblocked Diaphragm Altering S1 Range

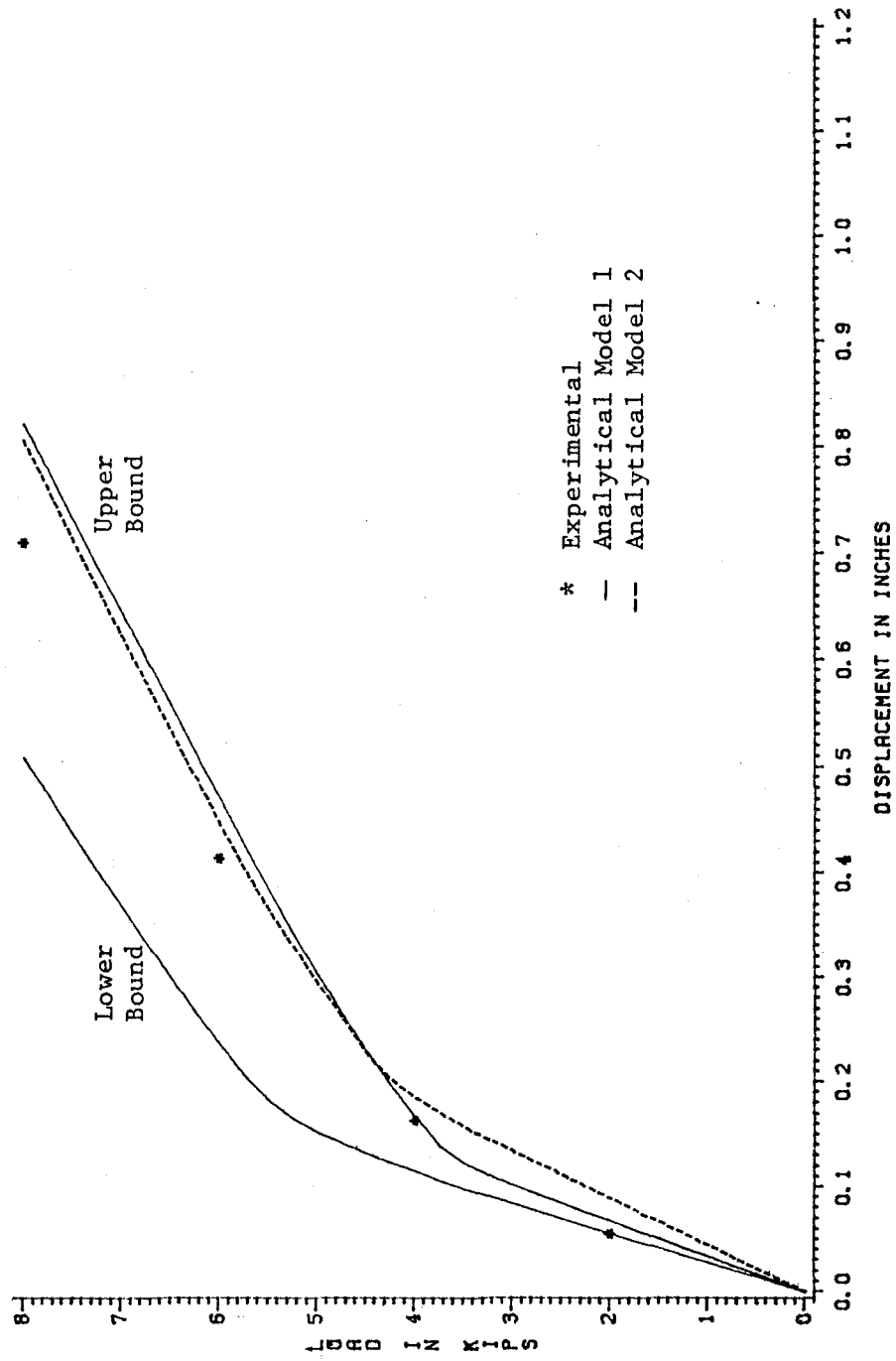


Figure 4.11 Displacement of Blocked Diaphragm

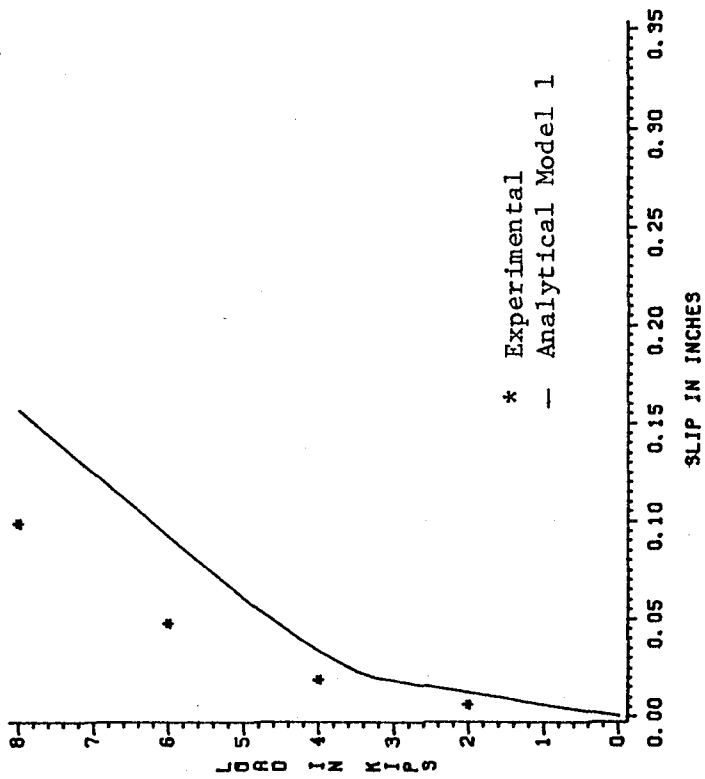


Figure 4.12 Slip at Position 3 of Blocked Diaphragm

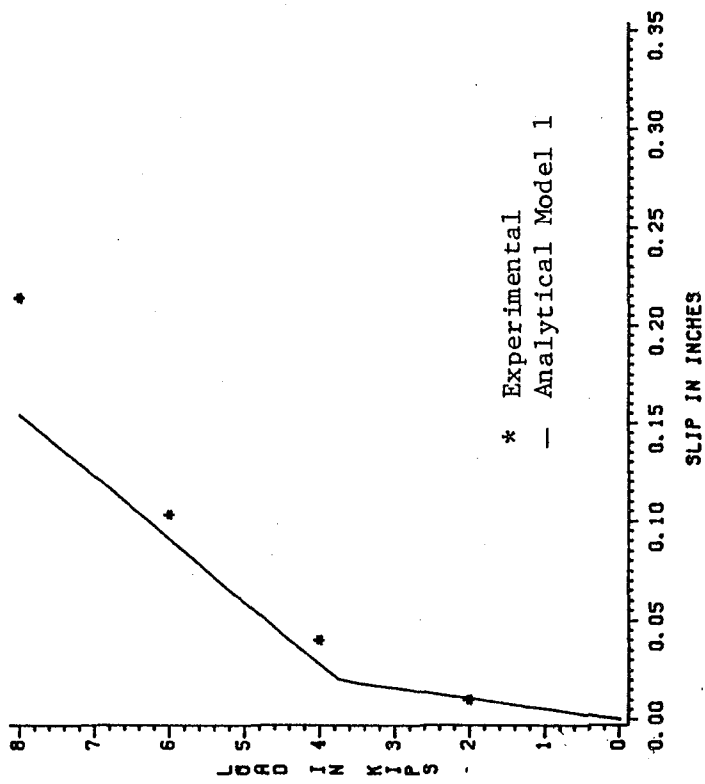


Figure 4.13 Slip at Position 4 of Blocked Diaphragm

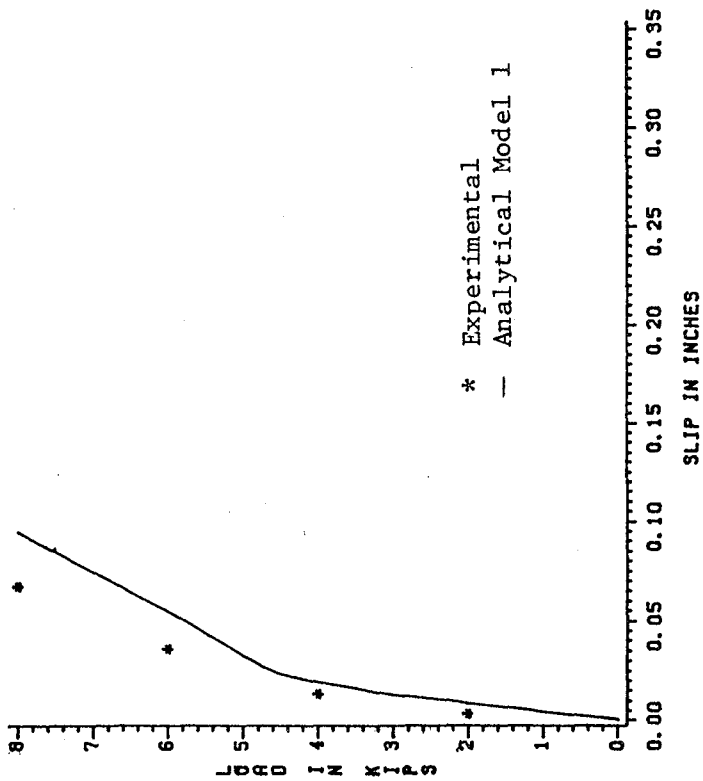


Figure 4.14 Slip at Position 6 of Blocked Diaphragm

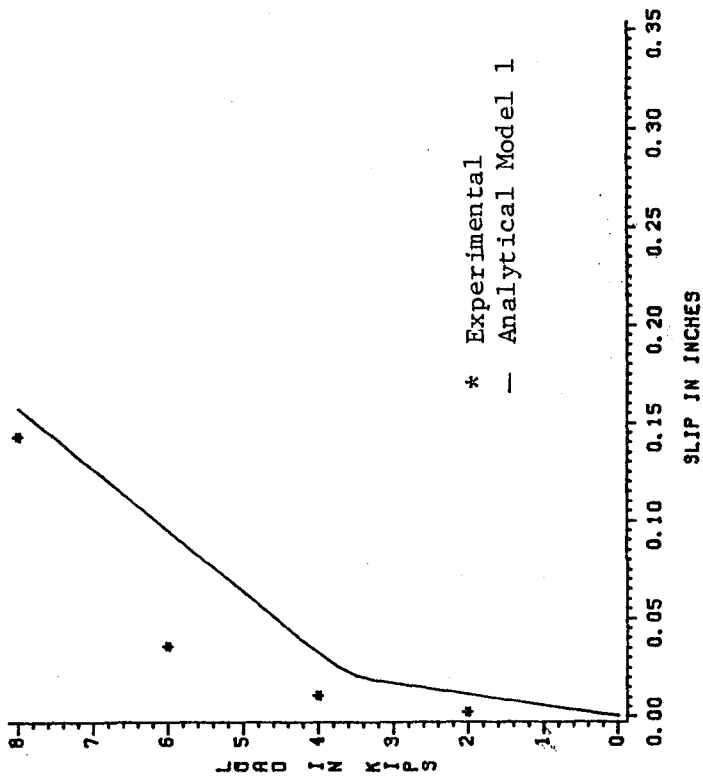


Figure 4.15 Slip at Position 7 of Blocked Diaphragm

4.8), which are between panel groups, are large relative to the slip at position 7 (Fig. 4.9), which is within a panel group.

Although the analytical model correctly predicts the general characteristics of the slip response, local slip behavior is not predicted adequately. For example, at points 1 and 5 (Fig. 4.8) the analytical transition from nail-slip stiffness S_1 to stiffness S_2 occurs at a smaller load than that indicated experimentally. A better correlation with experimental slip data was obtained by doubling the analytic transition load. However, the resulting effect on the global response was not acceptable (Fig. 4.10).

4.3.2 BLOCKED DIAPHRAGMS

The experimental diaphragm response for the blocked diaphragm is compared to the upper and lower bound results found considering nail-slip stiffness model 1 in Fig. 4.11. The upper bound results for nail-slip model 2 are also given.

A comparison of the results found using the different nail-slip models indicates behavior similar to that observed in the unblocked diaphragm except that the stiffness transition occurs at a load of four kips. This difference in transition load is attributed to the difference in nail spacing perpendicular to the joists, i.e., six inches in the blocked diaphragm versus sixteen inches in the unblocked diaphragm.

A comparison of the analytical and experimental results in Fig. 4.11 indicates that, in contrast to the unblocked diaphragm, the upper bound analysis yields a better prediction of observed response than the lower bound analysis. As a result, it may be concluded that toe-nailing does have an effect on nail-slip stiffness in the unblocked diaphragm. However, since the experimental response is stiffer than that predicted by the upper bound analysis, the actual decrease in nail effectiveness attributed to toe-nailing is probably less than the one-third reduction considered in this investigation. This

5. SUMMARY, CONCLUSIONS AND RECOMMENDATIONS

The results of an investigation into the in-plane shear behavior of plywood timber diaphragms have been presented. The particular focus of the study was on the response behavior to large cyclic deformations which may occur during an earthquake ground motion. The investigation involved both experimental and analytical phases. Summaries and conclusions from both the experimental and analytical phases are presented herein. Summaries and conclusions from each phase, as well as recommendations for additional research in this area, are presented in the following subsections.

5.1 EXPERIMENTAL PHASE

The experimental phase of the investigation involved two basic test series in which the behavior of 16 by 24 ft. full-scale plywood diaphragm models in response to various in-plane shear load histories was evaluated. In addition, small scale tests were carried out to evaluate local nail-slip response.

The results of the experimental phase, as well as various analytical results, clearly demonstrate that the in-plane shear response is controlled by the nail-slip characteristics of the joints between adjacent plywood panels, and between plywood panels and boundary elements. In other words, the diaphragm is analogous to a system of essentially rigid plates connected by flexible joints.

The diaphragm displacement response to monotonic shear force is initially linear, followed by a region in which the shear stiffness decreases gradually with increasing load (Fig. 3.1). Load reversal, after application of load into the nonlinear response region, results in a pinching phenomenon in the initial region of the force displacement response, characterized by a gradual increase in stiffness with load. Pinching is attributed to local damage to nailed joints caused during the previous load cycle. This damage results in "slack" in the joints which is recovered gradually as the load is increased (Fig. 3.1).

A comparison of the response of diaphragms with different blocking arrangements clearly indicates that blocking, placed along plywood panel boundaries perpendicular to the joists, significantly improves behavior. For example, the secant stiffness to a load of seven kips for the blocked and unblocked diaphragms compared in Fig. 3.8 increases by 100 percent (from 6.25 kips/in. to 12.5 kips/in.) when blocking is placed along plywood panel boundaries (referred to as the blocked diaphragm).

The improved behavior observed in the blocked diaphragm is attributed to the fact that nail spacing along plywood panel joints perpendicular to the joists was 6 in. as compared to 16 in. in the unblocked diaphragm. The closer nail spacing enhances the nail-slip mechanism along these joints, and consequently leads to a significant improvement in overall response.

The effect of increasing plywood panel thickness from 1/2 to 3/4 in. is another illustration of the significant influence of nail-slip response on overall behavior. The apparent initiation of shear degradation at a lower load, and the smaller overall strength (8 kips vs 10 kips) in the diaphragm with the thicker plywood indicates that response is controlled by nailed joint stiffness, which was adversely affected in this diaphragm due to a reduction in nail penetration depth.

The typical model failure was attributed to a rotation and subsequent separation of the closure boards at a corner joint. This failure mode, in conjunction with the excellent behavior of diaphragm VI in Test Series II which was reinforced to eliminate this mode of failure, demonstrates that, when large cyclic deformations are expected, care must be taken to ensure that locations of stress discontinuity do not limit the ability of the diaphragm to deform and resist load.

The need for careful detailing at stress discontinuities is also illustrated by the response of diaphragms with openings. In the diaphragm of Test Series I, shear transfer at the interior corner of the opening was not given

special consideration, resulting in relatively poor overall behavior. In Test Series II, however, this corner was detailed following the recommendations of ATC (21), and the observed behavior, with the exception of a 20 percent decrease in strength, was similar to that for diaphragms without openings.

5.2 ANALYTICAL PHASE

The analytical investigation has been carried out in two stages. The first stage was conducted by GangaRao and Luttrell (1979). A typical wooden diaphragm stiffened by joists has been idealized as a one- and two-dimensional structural element. The dynamic displacements and natural frequencies of one- and two-dimensional models are devised by including slip, damping effects, material properties, and varying boundary conditions.

Natural frequencies and displacements, computed from the abovesaid procedure (9) are compared with the finite element formulations and experimental values. The first term approximation of static displacements, computed from GangaRao and Luttrell procedure, are within 15 percent of the results obtained from the results from the finite element method. A closer comparison, within 5 percent, has been obtained by refining the finite element mesh. The anisotropic material properties and two-dimensional effects of the timber diaphragms are neglected in arriving at simple design equations. It has been found out, while stiffness of joists is predominant for natural frequencies parallel to joists, it practically has no effect on natural frequencies perpendicular to joists.

The one-dimensional idealization of wooden diaphragms clearly revealed that the damping of up to 30 percent of its critical value has little effect on the dynamic displacements and frequencies. Maximum damping coefficients of a "totally-failed" diaphragm were of the order of 15 to 20 percent of the critical value. Hence, the damping effects can be neglected in formulating simplified design equations for timber diaphragms. However, variation in slip-modulus

has a significant effect on the stiffness as well as natural frequency of a diaphragm. A simple design example of a plywood diaphragm bracing system under seismic forces is presented in the appendix of this report, along with the in-plane shear stiffness equations for blocked and unblocked diaphragms of varying nail spacing.

In the second stage, a finite element model in which plywood panels are idealized as substructures of isotropic, plane stress, quadrilaterals connected by dimensionless link elements included to represent nail slip, was developed. The experimental steel load frame is included in the model as a series of one-dimensional bar elements which are connected to the appropriate plywood panel substructure boundaries with nail-slip links. A bilinear nail-slip relationship is considered in the model, and an incremental, equilibrium-correcting tangent stiffness solution scheme was employed to solve the resulting nonlinear equilibrium equations.

The proposed finite element model predicts the general trends in the observed experimental, providing a reasonable prediction of overall diaphragm shear displacement behavior. The predicted local nail-slip response, however, does not adequately reflect experimental behavior and further refinement of the bilinear nail-slip idealization is required.

5.3 RECOMMENDATIONS

Although the results of this study demonstrate that properly detailed plywood diaphragms can perform satisfactorily when subjected to large cyclic deformations, which would be expected in response to a major earthquake ground motion, a number of unanswered questions remain. As a result, a number of recommendations for further study are made below.

1. The results of both the experimental and analytical phases of this investigation indicate the importance of nail-slip behavior in the cyclic response of plywood diaphragms. As

noted in the discussion of the analytical results in Chapter 4, the bilinear nail-slip model used in the finite-element model does not adequately predict local slip response. One problem with the nail-slip idealization considered in the analysis, is that the idealization is based on data for straight nailed joints. In the diaphragms tested, a number of panel joints were toe-nailed (i.e. nails driven at an angle to the surface) and a reduction of nail-slip stiffness is expected (25). In view of the lack of adequate nail-slip data for toe-nailed joints, an experimental investigation to quantify the reduction in nail-slip stiffness associated with toe nailing is recommended. Such a study would employ a small scale model of a typical interpanel nailed joint. In addition to the type of nailing, the influence of panel thickness, nail size, and load history - in particular the effect of large cyclic deformations - could be evaluated as part of the investigation.

2. The experimental results found in this investigation indicate that proper construction details, in particular details in areas of stress discontinuities, are necessary if diaphragm behavior in response to large cyclic deformations is to be satisfactory. In view of this observation, it is recommended that current construction practice be reviewed to identify typical design details at diaphragm corners, at openings, and in connections between the diaphragm and lateral load resisting elements such as masonry walls. A new experimental study of full scale plywood diaphragms would then be carried out to evaluate the adequacy of the various details in response to large cyclic deformation. The adequacy of details used for connections between floor diaphragms and lateral

load resisting elements is of particular concern, in view of the apparent failure of these connections in recent earthquakes (4).

3. The finite element model developed as part of this investigation is currently limited to monotonic load histories. Cyclic loading is expected, however, in response to an earthquake ground motion which is typically an important load condition in timber diaphragm design. As a result, it is recommended that model capabilities be extended to include cyclic loading. This extension would involve a modification of the idealized nail-slip relationship to reflect the cyclic degradation in shear stiffness observed in the experimental response. Of particular concern is the pinching phenomenon. The extension to cyclic loading should be carried out in conjunction with the detailed experimental evaluation of cyclic nail-slip response described in the first recommendation.

4. As noted in the discussion of the analytical results, the relatively coarse finite element mesh required to adequately model the shear deformation response of a typical plywood panel indicates that the current substructure panel model may not be the most efficient. In view of this observation, it is recommended that a new model in which a typical panel is idealized as a variable noded quadrilateral (4 to 9 nodes) be formulated, and evaluated with respect to accuracy and solution time.

5. After completing recommendations 3 and 4, the basic diaphragm model could be incorporated as an element in a general analysis program. Using this program, in which the supporting frame elements would be idealized and defined as

diaphragm boundaries, the response of building structures with timber diaphragms to various lateral load conditions, including dynamic loading associated with earthquake ground motion, could be evaluated.

REFERENCES

1. Vanderbilt, M.D., J.R. Goodman, M.E. Criswell, and J. Bodig, "A Rational Analysis and Design Procedure for Wood Joist Floor Systems," Final Report to the National Science Foundation, Colorado State University, Fort Collins, Colo., 1974.
2. Thompson, E.G., J.R. Goodman, and M.D. Vanderbilt, "Finite Element Analysis of Layered Wood Systems," Journal of the Structural Division, ASCE, vol. 101, No. ST12, 1975, pp. 2659-2672.
3. Schaefer, E.M. and M.D. Vanderbilt, "Comprehensive Analysis Methodology for Wood Floors", Journal of the Structural Division, ASCE, Vol. 109, No. 7, July, 1983, pp. 1680-1694.
4. Spangler, B.D., "Field Performance of Wood Diaphragms in Structures Subjected to Wind Forces," Proceedings of a Workshop on Design of Horizontal Wood Diaphragms, Applied Technology Council, Publication ATC-7-1, November 1979.
5. Gray, G.W., "Field Performance of Wood Diaphragms in Structures Subjected to Seismic Forces," Proceedings of a Workshop on Design of Horizontal Wood Diaphragms, Applied Technology Council, Publication ATC-7-1, November 1979.
6. Jewell, R.B., "The Static and Dynamic Experimental Analysis of Wooden Diaphragms," M.S. Thesis, Department of Civil Engineering, West Virginia University, August 1981.
7. Corda, D.N., "The In-Plane Shear Response of Timber Diaphragms," M.S. Thesis, Department of Civil Engineering, West Virginia University, June 1983.
8. Roberts, J., "Finite Element Analysis of Horizontal Timber Diaphragms," M.S. Thesis, Department of Civil Engineering, West Virginia University, Morgantown, W.V., 1983.
9. GangaRao, H., and Luttrell, L.D., "Preliminary Investigation into the Response of Timber Diaphragms," Proceedings of a Workshop on Design of Horizontal Wood Diaphragms, Applied Technology Council, Publication ATC-7-1, November 1979.
10. Tottenham, H., The Effective Width of Plywood Flanges in Stressed Skin Construction, 1970.
11. Bower, W.H., "Lateral Analysis of Plywood Diaphragms," Journal of the Structural Division, ASCE, Vol. 106, September 1980, pp. 759-772.
12. Gulkan, P., R.L. Mayes and R.W. Clough, "Strength of Timber Roof Connections Subjected to Cyclic Loads," Earthquake Engineering Research Center, Report No. UCB/EERC-78/17, September 1978.

13. Uniform Building Code, International Conference of Building Officials, Whittier, California, 1976.
14. Ewing, R.D., T.J. Healey, and M.S. Agbabian, "Seismic Analysis of Wood Diaphragms in Masonry Buildings," Proceedings of a Workshop on Design of Horizontal Wood Diaphragms, Publication ATC-7-1, November 1979.
15. Kuenzi, E.W., "Theoretical Design of Nailed or Bolted Joints Under Lateral Load," U.S. Department of Agriculture, No. F, 1951, September 1953.
16. Wilkinson, T.L., "Theoretical Lateral Resistance of Nailed Joints," Journal of the Structural Division, ASCE, Vol. 98, pp. 2005-2013, January 1971.
17. Wilkinson, T.L., "Analysis of Nailed Joints With Dissimilar Materials," Journal of the Structural Division, ASCE, Vol. 98, pp. 2005-2013, January 1971.
18. McLain, T.E., "Curvilinear Load Slip Relations in Laterally Loaded Nail Joints," thesis presented to Colorado State University at Fort Collins, Colorado in 1975, in partial fulfillment of the requirements for the degree of Doctor of Philosophy.
19. Stone, J.L., "Generalized Load-Slip Curve for Nailed Connections," thesis presented to Colorado State University, at Fort Collins, Colorado in 1980, in partial fulfillment of the requirements for the degree of Master of Science.
20. Antonides, C.E., "Interlayer Gap Effects on Nail Slip Modulus," thesis presented to Colorado State University, at Fort Collins, Colorado in 1979, in partial fulfillment of the requirements for the degree of Master of Science.
21. Applied Technology Council, "Guidelines for the Design of Horizontal Wood Diaphragms", ATC-7, 1979, Applied Technology Council, Palo Alto, CA.
22. American Plywood Association, Plywood Diaphragm Construction, Tacoma, Washington, 1970.
23. Forest Products Laboratory, Forest Service, U.S. Department of Agriculture, Wood Handbook: Wood as an Engineering Material, Agriculture Handbook No. 72, August 1974.
24. Douglass Fir Plywood Association, "Design of Flat Plywood Stressed Skin Panels," DFPA Design Method No. Ss-62D, Tacoma, Washington, May 1962.
25. Gurfinkel, G., Wood Engineering, Southern Forest Products Association, 1973.
26. "American National Standard Minimum Design Loads for Buildings and Other Structures," ANSI A58.1-1982, Revision of ANSI A58.1-1972.

Appendix

The design of a plywood diaphragm bracing system requires that its shear strength and shear stiffness be known. It must be sufficiently strong to resist applied loads and to resist them within specific deflection limits. Further, the fundamental elastic period of vibration T must be established for finding seismic forces.

For seismic loading cases for example, ANSI A58.1-1982 (26) sets out minimum lateral seismic forces as:

$$\begin{array}{ll} \text{where:} & V = ZIKCSW \quad (A-1) \\ & Z = \text{Zone Coefficient} \\ & I = \text{Occupancy Factor} \\ & K = \text{Horizontal Force Factor} \\ & C = 1/(15T^{0.5}) \\ & S = \text{Soil Factor} \\ & W = \text{Dead Load} \end{array}$$

The distinction for the diaphragm type is in the fundamental period T which can be in the general form

$$T = 2\pi (M \cdot \Delta/P)^{0.5} \quad (A-2)$$

$$\begin{array}{ll} \text{where:} & M = \text{Assigned Tributary Area Mass} \\ & P/\Delta = \text{System Stiffness} \end{array}$$

The stiffness assessment depends on shear distortion within panels and, especially, on joint slip related to average shear forces on nails along any joint.

A typical diaphragm zone, representing a full roof diaphragm, can be examined as in Figure A-1. Two effects of nail slip are dominant. Under direct shear, two adjacent elements can slip δ_i as shown. Further, following Figure A-1b, horizontal slips manifest themselves in a further relaxation δ_r :

$$\delta_r = \frac{w}{b} (eht + ehb)$$

If there are N sub-panels across the width A , then $N-1$ interior joints are present even if staggered joints are used. Then, due to nail slip,

$$\Delta_s = (N-1)S_i + 2\delta_o + N\frac{w}{b} (eht + ehb) \quad (A-3)$$

$$\text{where:} \quad \delta_o = \text{Nail Slip Along the B Dimension at Edges}$$

If consistent nail spacings are used on all supports across the diaphragm, $eht = ehb = e_x$. Since δ_i on interior joints represents relative movement between two units, $\delta_i = 2e_y$.

The direct shear distortion within the sheets can be expressed in terms

of P/Gt where G is the sheet shear rigidity and t is the effective thickness.

Then the total deflection at P from direct shear distortion and nail slip is,

$$\Delta = \frac{A}{B} \frac{P}{Gt} + 2(N - 1)e_y + 2\delta_0 + N \frac{w}{b} (2e_x) \quad (A-4)$$

Along the principal slip lines, parallel to B , a total force Z must be transferred in the vicinity of each joist as in Figure A-2. Considering the end-most joists to transmit only a $Z/2$ force,

$$Z = \frac{P}{12B/J} = \frac{P}{0.75B}$$

where: $J =$ Joist Spacing (16" in this application)

For equilibrium to develop across the sheet width w at a joist, the nail shears Q_i must satisfy:

$$\Sigma Q_i X_i = Zw$$

using a linear distribution across w , $Q_i = Q \left(\frac{X_i}{w/2} \right)$

$$\text{Then } Q = \frac{Z}{2} \frac{1}{\Sigma (x^2/w^2)} = \frac{P}{1.5B \Sigma (x^2/w^2)} \quad (A-5)$$

If blocking is used under these joints such that m pairs of nails may be used between joists,

$$Q = \frac{P}{1.5B \Sigma (x^2/w^2) + 0.75Bm} \quad (A-6)$$

Noting the equilibrium of the diaphragm in Figure A-1, the shear force along the A dimension is

$$R = \frac{A}{B} P$$

Letting the nail spacing, along the A edge be S_A inches, the average shear force per nail is $RS_A/12A$ and

$$N_{ex} = \frac{NR}{12KA} S_A = \frac{NP}{12KB} S_A$$

where K is the nail shear stiffness in lbs/inch.

Similarly, with S_B being the nail spacing, in inches, along the edges parallel to B

$$2e_{yo} = \frac{2P}{12KB} S_B$$

Then the general deflection equation can be rewritten with $w/b = 1/2$ for typical plywood sizes:

$$\frac{\Delta}{P} = \frac{A}{B} \cdot \frac{1}{Gt} + \frac{1}{BK} \left(\frac{2(N-1)}{1.5 \Sigma x^2/w^2 + 0.75M} + \frac{1}{6} S_B + \frac{N}{12} S_A \right) \quad (A-7)$$

For 4" nail spacing across a 48" width W,

$$\Sigma x^2/w^2 = 2(4^2 + 8^2 + 12^2 + 16^2 + 20^2 + 24^2)/48^2 = 1.2639$$

And, for a 6" spacing,

$$\Sigma x^2/w^2 = 2(6^2 + 12^2 + 18^2 + 24^2)/48^2 = 0.9375$$

For most of the cases tested, the diaphragms had $A = 16'$ and $N = 4$. For example, using a 4" nail spacing throughout,

$$\frac{\Delta}{P} = \frac{16}{B} \frac{1}{Gt} + \frac{1}{BK} \left(\frac{6}{1.896 + 0.75m} + 2 \right) \quad (A-8)$$

With blocking under joints between joists, the use of nails at 4" spacing leads to $m = 3$ (with no blocking, use $m = 0$) and,

$$\frac{\Delta}{P} = \frac{16}{B} \frac{1}{Gt} + \frac{1}{BK} (3.447)$$

For No. 8 nails, $K = 10,000$ lbs./inch. Further the plywood shear rigidity is about 10^5 lbs./inch and half-inch plywood has an equivalent thickness of 0.316 inches. If B is taken at 24 feet as in certain tests,

$$\frac{\Delta}{P} = \frac{16}{24} \frac{1}{0.316 \times 10^5} + \frac{3.447}{24 (10^4)} = 35.5 \times 10^{-6} \frac{\text{in.}}{\text{lb.}} \quad (A-9)$$

This corresponds to a stiffness $P/\Delta = 28,000$ lb./in. which is very typical of measured initial stiffnesses. A typical system tested had a mass^M of about 105 lb.-sec²/ft. Then for the cantilevered diaphragm with only one edge moving, the initial period would be about

$$\begin{aligned} T &= 2\pi \sqrt{0.5M (\Delta/12P)} \\ &= 2\pi (0.5 \times 105 \times 35.5 \times 10^{-6}/12)^{0.5} = 0.078 \text{ sec.} \end{aligned} \quad (A-10)$$

the period T is critical to finding the C term for Equation A-1.

Example:

A single story retail building, Figure A-3, has $H = 25'$, $B = 86'$, and $L = 180'$. The Δ/P value from Equation A-9 is considered as typical for the roof. Further, the roof weighs 12 psf and the walls at 15 psf, depend on the roof diaphragm for lateral support. Follow ANSI A58.1 and find the maximum shear delivered to the B end wall along line a - c.

Zone 2.

$$Z = 3/8$$

$$K = 1.0$$

$$I = 1.25 \text{ (shopping center)}$$

$$S = 1.0 \text{ (soil type S1)}$$

A one-foot strip of the roof support zone has a weight of

$$W = 2\left(\frac{H}{2}\right) (15) + 86(12) = 1407 \text{ lbs./ft.}$$

Then from Equation A-2,

$$T = 2\pi\left(\frac{1407}{32.2} \cdot \frac{35.5}{10^6} \cdot \frac{1}{12}\right)^{0.5} = 0.0114 \text{ sec.}$$

$$C = 1/(15T^{0.5}) = 0.624$$

$$KCS = 0.624 \text{ and}$$

$$V = (3/8) (1.25) (0.624) (1407) = 412 \text{ lbs./ft.}$$

Then with V acting in the roof plane and along the full length L , the maximum shear force delivered at line ac is

$$R = 412(L/2) = 37080 \text{ lbs.}$$

The average maximum design shear is $R/B = 431 \text{ lbs./ft.}$

The average maximum design shear of 431 lbs./ft. is somewhat on the high side for the resistance of three nails per foot along the diaphragm edge at the wall. This effect can be minimized through substructuring or providing braced frames.

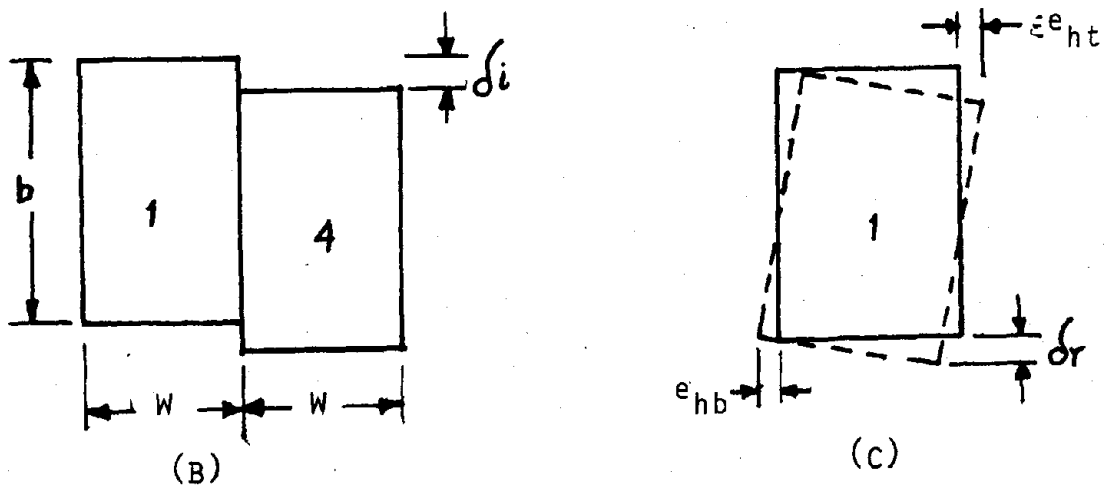
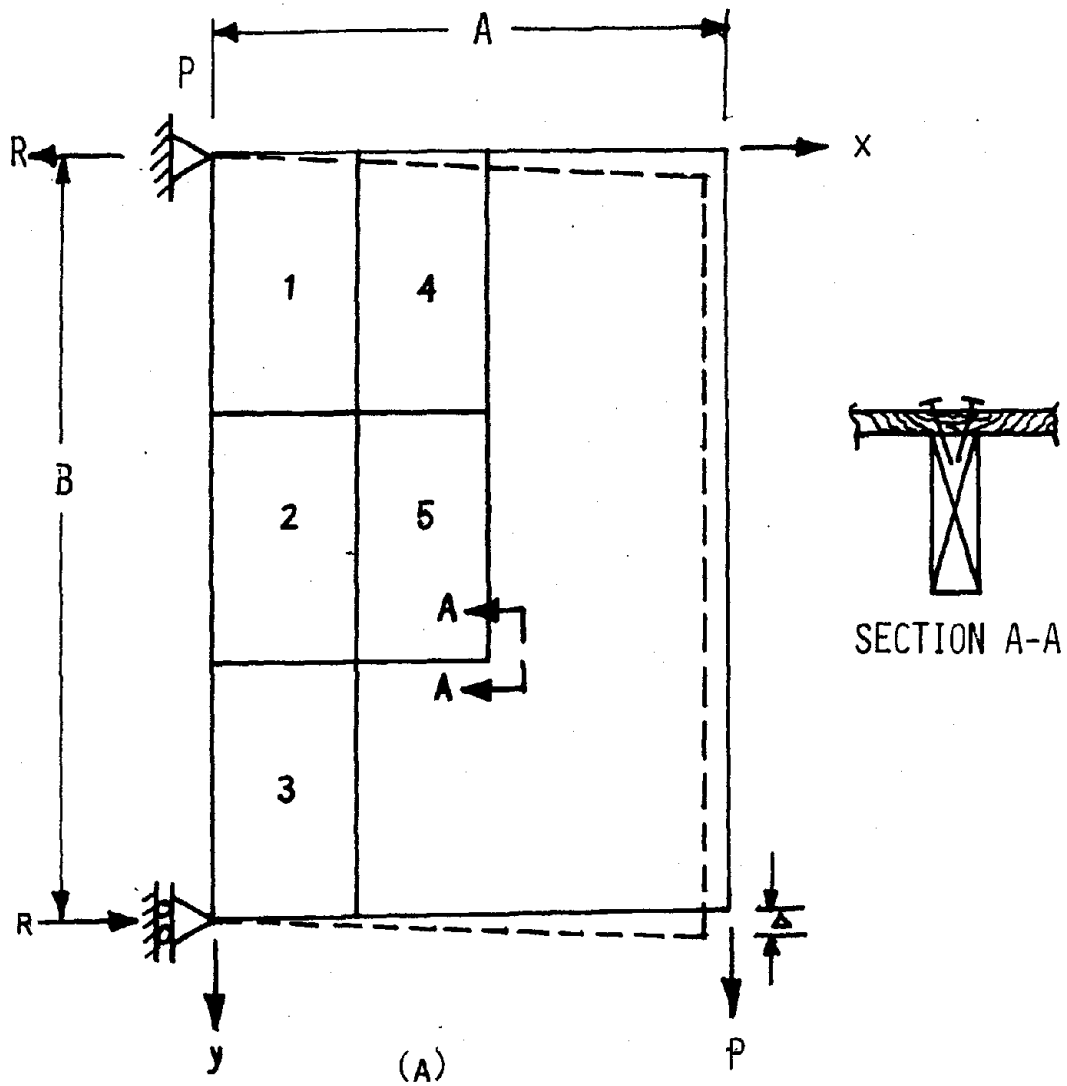


FIGURE A-1. - DIAPHRAGM LAYOUT

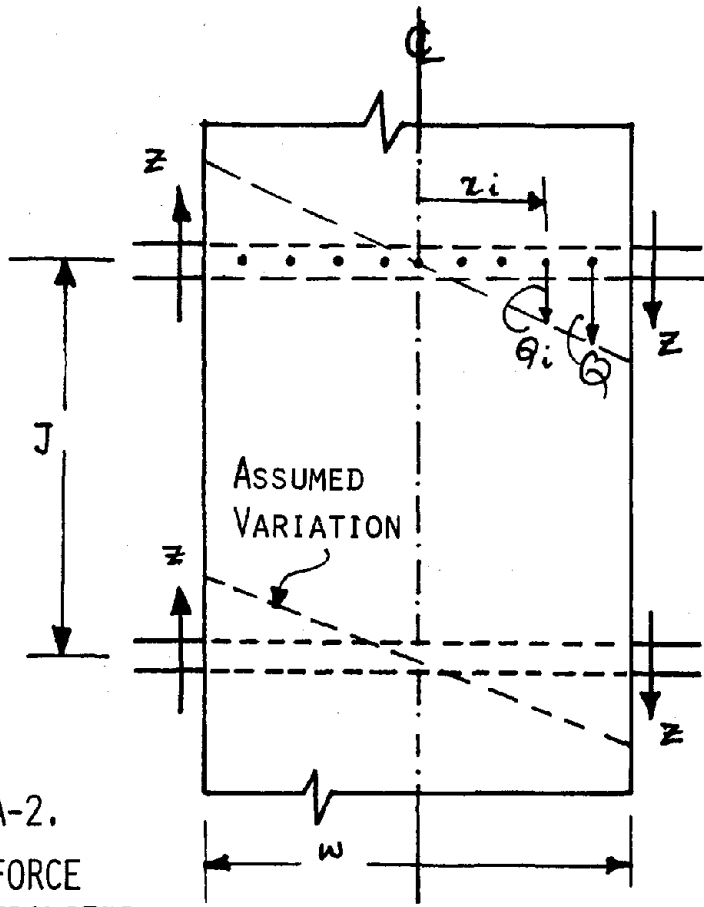


FIG. A-2.
FORCE
TRANSFER

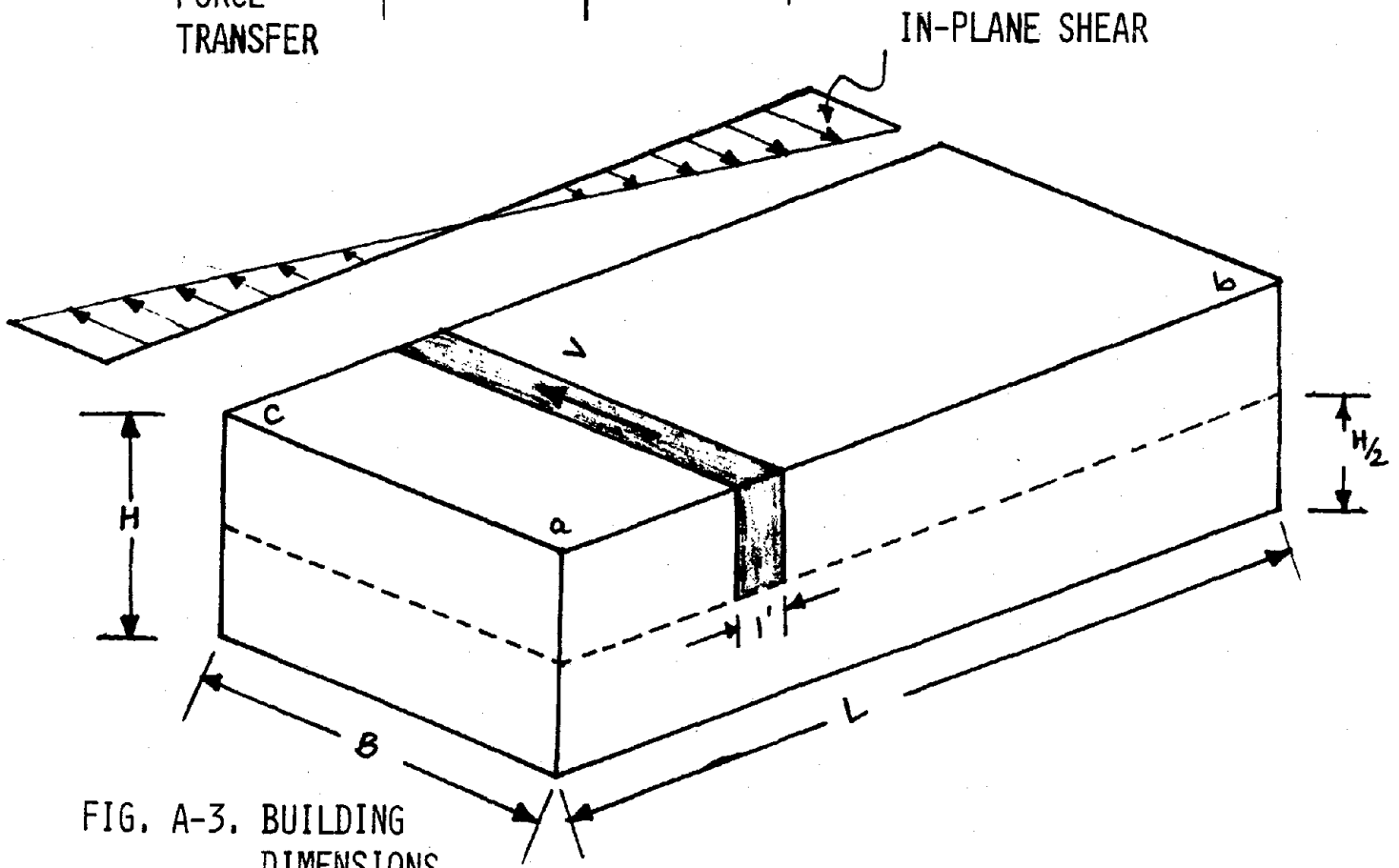


FIG. A-3. BUILDING
DIMENSIONS